"BABEŞ-BOLYAI" UNIVERSITY OF CLUJ-NAPOCA

FACULTY OF PHYSICS

PhD Thesis

"Magnetocaloric effect in rare earth-3d transition metal intermetallic and oxidic compounds"

Scientific coordinator

Prof.Dr. Romulus Tetean

PhD. Student

Adrian Bezergheanu

Cluj-Napoca 2012

Many events related to the coupling of magnetic sublattices with an external magnetic field can be triggered by varying the latter around a solid. This include the magneto-thermodynamic phenomenon known as the magnetocaloric effect (MCE). This is defined as the heating or cooling (i.e., the temperature change) of a magnetic material due to the application of a magnetic field. This effect has been called adiabatic demagnetization for years, though this phenomenon is one practical application of the MCE in magnetic materials.

In our days there is a great deal of interest in using the MCE as an alternative technology for refrigeration, from room temperature to the temperatures of hydrogen and helium liquefaction (~ 20-4.2 K). The magnetic refrigeration offers the prospect of an energy-efficient and environment friendly alternative to the common vapor-cycle refrigeration technology in use today.

The complex physical properties of this type of materials are very interesting both, from fundamental and technical point of view. Many of these properties are not well describe by theoretical models because of the complexity of interactions which are involved. There are necessary magnetic fields on the order of 2-5 T which can be produced now in a simply way using superconducting coils. In the same time high enough magnetic fields can be produce with new discovered high specific energy Nd-Fe-B permanent magnets. MCE in paramagnets (PM) was used as the first practical application, the so-called adiabatic demagnetization. With this technique, ultra-low temperatures can be reached (mK-μK).

In order to achieve good results I have to start with theoretical calculations, preparation and characterization of the samples, and finally interpreting the data and publish.

For samples preparation we shall use different techniques. The intermetallic compounds will be prepared by arc melting in argon atmosphere method, levitation method, mechanical alloying and the perovskite samples that were prepared by standard ceramic reaction at high temperatures. The purity of the starting materials was (99.99%) delivered by the company Alfa Aesar, Jonson & Matthey, Karlsruhe, Germany. The thermal treatment will be done in different conditions using furnace with controlled temperature and atmosphere. The structure and morphology of the samples will be studied by X-ray diffraction using a Bruker 8 XD diffractometer at the Faculty of Physics, Babes-Bolyai University. The magnetization measurements were performed using a commercially built *Cryogenic Free Vibrating Sample Magnetometer*, located at the "*Ioan Ursu Institute*" – *Faculty of Physics*,

Cluj-Napoca. The *VSM* includes a cryostat that allows measurements in the *1.6 - 700 K* temperature range and fields up to *12T*.

The main objective of this research is to find new materials which exhibit large magnetocaloric effect with high refrigeration capacity. There are many groups of researchers working in this field from European Union, United States, Japan, China etc. After our knowledge there are no other groups in our country working in this area.

An important objective is to lower the production costs of this materials having in mind that rare-earth metals are very expensive. With respect to this objective we shall compare the results (i.e. magnetic entropy variation, the adiabatic temperature change and the refrigeration capacity) considering different ways of preparation, thermal treatments and the morphology of the compounds. The research will be focused in main directions: magnetocaloric effect in intermetallic compounds rare earth 3d transition metal and oxidic compounds. The issues to be solved in this thesis are to find no so expensive materials with large refrigeration capacity in not so high magnetic fields, easy to be prepared and safe from environmental point of view. In order to achieve these objectives we shall prepare different classes of materials with transition temperatures in the range 20-350 K.

The proposed objectives of this thesis are focused on a better understanding of the physical phenomena involving in the magnetocaloric effect, which is very important from basic research point of view in interconnection with other priorities like nanoscience and materials. The proposed objectives are included in technological platform: Advanced engineering materials and technologies materials.

Chapter1

1.1. Short history

The magnetocaloric effect (MCE) is defined as the heating or cooling (in the temperature change) of a magnetic material due to the application of a magnetic field. This effect has been called adiabatic demagnetization for years, though this phenomenon is one practical application of the MCE in magnetic materials. Another definition: is the thermal response of a magnetic material to an applied magnetic field and is apparent as a change in its temperature. In 1881 Warburg discovered the magnetocaloric effect when observed it in iron [1]. After few years in 1926 the origin of this effect was explained independently by Debye [2] and Giaque [3]. They also suggested the first practical use of the magnetocaloric effect (the adiabatic demagnetization) used to reach temperatures lower than that of liquid helium by using the magnetocaloric effect of paramagnetic salts. Giaque and MacDougall have put this idea in practice in 1933 and they experimentally demonstrated the use of magnetocaloric effect to achieve temperatures below 1K [4]. One of the emerging challenges after 1933 was to use this effect to develop applications at higher temperature. In 1976 Brown reported a prototype of room-temperature magnetic refrigerator and demonstrates that magnetic refrigeration is possible in room-temperature range [5]. Nowadays is a great interest to use the magnetocaloric effect as technology for refrigeration from the room-temperature to the temperature of hydrogen or helium liquefaction (20-4,2K).

1.2. Magnetic behavior of matter.

Atomically, the magnetism of solids originates nearly exclusively from electrons. Nuclear moments contribute very little to the magnetization but are important, for example, in resonance imaging. The magnetic moment of the atom is given by the sum of spin and orbital magnetic moments of the electrons. One electron per atom corresponds to an atomic moment of one Bohr magnetron ($1\mu_B = 9.274\times10^{-24}$ J/T)

1.3. Main classes of magnetic behaviour:

1.3.1. Diamagnetism, 1.3.2. Paramagnetism, 1.3.3. Magnetic ordered substances.

1.4. Magnetocaloric effect

All the magnetic materials present a magnetocaloric effect. The effects depend of the properties of each material. In the case of magnetic materials, the materials heats up when a magnetic field is applied and cool down when the magnetic field is shut down. The value of magnetocaloric effect is characterized by the adiabatic temperature change ΔT_{ad}, or by the entropy change ΔS_{ad} while varying the magnetic field. The technology of magnetic

refrigeration is based on the magnetocaloric effect. Magnetic refrigeration is an environment alternative to the common vapour-cycle refrigeration technology used today [6,7]. The many modern refrigerators and air conditioning systems have harmful effects like "ozone depleting" or "global warming".

1.4.1 Base theory of magnetocaloric effect (MCE)

Magnetocaloric effect can be explained using thermodynamics. One of the thermodynamic parameter is C_P and will be explain latter in first order transition [8]. The thermodynamics explain the entropy and temperature change dependences of magnetic variables (magnetization and magnetic field). The magnetocaloric effect is the result of entropy variation given by the coupling of magnetic spins system with the magnetic field. We can make the equivalence with thermodynamics of a gas.

- isothermal compression of a gas (when temperature is kept constant and a pressure is applying it can be observe the changes of the entropy, it decrease) is analogous to the isothermal magnetization of a paramagnet or a soft ferromagnet (when is applying a magnetic field, the magnetic entropy decreases)
- adiabatic expansion of a gas (when the entropy is constant and the pressure is decreasing the result is the modification of temperature, that means decreasing of temperature) this process is equivalent with adiabatic demagnetization (decreasing the magnetic field to zero, the entropy remains constant and the value of temperature decreases until the magnetic entropy increase) . The total entropy of a magnetic material is given by the equation:

$$S(T,\mathbf{H}) = S_m(T,\mathbf{H}) + S_{lat}(T) + S_{el}(T)$$

For the magnetic materials which present magnetocaloric effect the value of magnetic entropy S_m must be higher. For study the magnetocaloric effect the magnetic entropy change ΔS_m is the most important characteristic of a magnetic material.

The magnetocaloric effect is totally characterized when the total entropy of a magnetic material is given as a function of both magnetic field and temperature.

Chapter 2. MCE characterization

2.1. Determination of the magnetocaloric effect

2.1.1Direct measurements. This direct method to measure MCE is based on measurements of initial temperature (T_0) and finale temperature (T_F) of the material when the magnetic field varies from an initial value (H_0) to a final value (H_F). The value of adiabatic temperature is given by the relation: $\Delta T_{ad}(T_0,\mathbf{H_F}\text{-}\mathbf{H_0}) = T_F - T_0$ Considering all these effects, the accuracy is between 5-10% [9, 10].

2.1.2.Indirect measurements. The indirect measurements allow the calculation of both $\Delta T_{ad}(T,\Delta H)$ and $\Delta S_m(T,\Delta H)$ in the case of heat capacity measurements or in the case of magnetization measurements. In the second case the magnetization must be measured as a function of T and H [11]. The accuracy of the indirect measurements to calculate the magnetic entropy change $\Delta S_m(T,\Delta H)$ depends of the measurements accuracy of magnetic moments. The error range is 3-10%. The entropy of a solid can be calculated from the heat capacity using the relations:

$$S(T)_{H=0} = \int_0^T \frac{C(T)_{P,H=0}}{T} dT + S_0 \quad \text{and} \quad S(T)_{H\neq 0} = \int_0^T \frac{C(T)_{P,H}}{T} dT + S_{0,H}$$

2.2 Magnetocaloric effect in paramagnets

In paramagnets MCE was used as the first practical application, the so-called adiabatic demagnetization. Using the magnetocaloric effect as a refrigeration technique, ultra-low temperatures can be reached (mK-μK). In the year 1927, Giauque and MacDougall [3, 4] showed with there pioneer work that using the paramagnetic salt $Gd_2(SO_4)_3 \cdot 8H_2O$, it could be reached T lower than 1 K. After a while, MCE at low temperatures was studied in other paramagnets salts, such as ferric ammonium alum $[Fe(NH_4)(SO_4) \cdot 2H_2O]$ [12], chromic potassium alum [13] and cerous magnesium nitrate [14]. For the practical application of adiabatic demagnetization using paramagnetic salts the difficulty lies in its low thermal conductivity. Therefore, the study of paramagnetic intermetallic compounds was the next step in this practical application. $PrNi_5$ was one of the most studied materials and it is actually used also today in nuclear adiabatic demagnetization devices. The lowest temperature: 27μK has been reached using $PrNi_5$ [15].

2.3 Magnetocaloric effect in order-disorder magnetic phase transition

Under a certain temperature in solid state spontaneous magnetic ordering of paramagnets is a cooperative phenomenon. The ordering temperature depends on the strength of exchange interaction and on the nature of the magnetic sublattice in the material. When spontaneous magnetic ordering takes place, the magnetization strongly varies in a very narrow temperature range in the closeness of the transition temperature, (the Néel temperature for antiferromagnets and the Curie temperature for ferromagnets or ferrimagnets. The fact that $\left[\frac{dM}{dT}\right]_H$ is large gives the possibility these magnetic materials to have a significant magnetocaloric effect. The

maximum magnetic entropy for a lanthanide is $\Delta S_m = R\ln(2J+1)$, where R represents the universal gas constant and J is the total angular momentum. Rare-earth metals or lanthanides (4f metals) and their alloys have been much more considerably studied than 3d transition metals and their alloys, because the available magnetic entropy in rare earths is extensively larger than in 3d transition metals. So that it can be obtain a large magnetocaloric effect the derivative magnetization with respect to temperature must be large because it is not the absolute value of the magnetization that is important.

2.4 Magnetocaloric effect in first order magnetic phase transition and the giant effect

The existence of short-range order and spin fluctuations above the order temperature (T_C) in second-order magnetic phase transitions brings about a reduction in the maximum possible $\left[\frac{dM}{dT}\right]_H$ value, and the maximum MCE is accordingly depressed. Different from that, a first-order phase transition ideally happens at constant temperature (the transition temperature, T_t) and thus the value $\left[\frac{dM}{dT}\right]_H$ should be infinitely large. To be more precise, in an ideal first-order phase transition, the discontinuity in both magnetization M and entropy S causes that the derivatives in the mostly used Maxwell must be replaced by the finite increments of the Clausius-Clapeyron equation for phase transformations. The discontinuance in the entropy is related to the enthalpy of transformation, which is also known as latent heat. The first-order transition takes place if the two magnetic phases have equal thermodynamic potential.

An extra contribution to MCE, yielding the so-called giant magnetocaloric effect is brought out by the existence of this entropy change associated with the first-order transition. Regretfully the giant effect can not be reversed, and giant MCE can only be observed in samples only one time (for new applications of magnetic field the temperature change haven't such big value). Following the outburst caused by the discovery of a giant MCE in $Gd_5(Si_xGe_{1-x})_4$ intermetallic alloys, ample research is being undertaken to find new intermetallic alloys showing first-order field-induced phase transitions, which is in general associated with a strong magnetoelastic coupling.

2.5 Magnetic refrigeration

In ours days there is a great deal of interest in utilizing the MCE as an alternate technology for refrigeration both in the ambient temperature and in cryogenic temperatures. Magnetic refrigeration is an environmentally friendly cooling technology. It does not use ozone-

depleting chemicals (such as chlorofluorocarbons), hazardous chemicals (such as ammonia), or greenhouse gases (hydrochlorofluorocarbons and hydrofluorocarbons).

Ozone-depleting or global-warming volatile liquid refrigerants are still used in the most modern refrigeration systems and air conditioners. An important difference between modern refrigeration systems and magnetic refrigerator is described by the refrigeration components.

Even the newest most efficient commercial refrigeration units operate well below the maximum theoretical (Carnot) efficiency, further improvements may be possible with the existing vapor-cycle technology. Magnetic refrigeration, however, because it offers considerable operating cost savings by eliminating the most inefficient part of the refrigerator: the compressor is rapidly becoming competitive with conventional gas compression technology. We can generate magnetic fields around 2T by permanent magnets. The researching is based on magnetic materials which showing significant magnetocaloric effect at these values of magnetic field.

The heating and cooling that occurs in the magnetic refrigeration technique is proportional to the size of the magnetic moments and to the applied magnetic field. This is why research in magnetic refrigeration is at present almost exclusively conducted on superparamagnetic materials and on rare-earth compounds. Refrigeration in the subroom temperature (~250K-290K) range is of particular interest because of potential impact on energy savings and environmental concerns.

Chapter 3. Sample preparation

3.1. Arc melting furnace, 3.2. RF melting furnace, 3.3. Mechanical alloyng.

Samples were prepared by melting constituent elements. Melting method was used in an electric arc furnace in the Laboratory of Physics of Babes-Bolyai University from Cluj-Napoca. To ensure a better mixing of the compound the samples were remelted several times then followed a heat treatment for several days at high temperature. For sample preparation we used high-purity substances over 99.9%. There is anather method to abtain alloys. This second method used RF melting furnace. Induction heating is based on the penetration of the electromagnetic energy in a solid conductor situated in a variable magnetic field in time of a coil (inductor). Conductor heating effect is produced by the Joule-Lenz low of induced currents swirl. A diversification requirement that must be fulfilled magnetic materials has lead to improved methods to obtaining them. Thus one of these procedures for obtaining nanocomposite materials include mechanical alloying and grinding, respectively.

Being among the latest technique for obtaining magnetic materials alloying and mechanical milling allows us to obtain microstructures with specific magnetic properties. For experiments alloying and mechanical milling, the most commonly used in laboratories are planetary mills Fritsch or Rech type. The powders of the materials are placed in bowls together whit balls for grinding process. To avoid oxidation the bowls are usually loaded with powders of the materials in different atmosphere (argon, helium, nitrogen) or vacuum.

Chapter 4. Structural and magnetic investigation

4.1 X-ray diffraction. After preparation, the crystallographic structure of all investigated samples was checked at room temperature using X-ray powder diffraction data. The structural characterization was made using a Bruker D8 Advance diffractometer**,** belonging to "*Ioan Ursu Institute*", Faculty of Physics, from Babes-Bolyai University, which can be used for almost all applications involving X-ray diffraction, including the structure finding, phase analysis, tension stress measurements, and texture measurements. The main parts of the diffractometer are: goniometer, X-rays tube, scintillation detector, sample holder, monochromator. By plotting the intensity against the angle of the incident X-ray, we can produce a series of peaks. The acquired data were analyzed using *PowderCell 2.3*.software [16].

4.2 Magnetic properties. *Vibrating Sample Magnetometer – VSM*, based on *Faraday*'s law, represents by far the most commonly used magnetometer, both in scientific and production area, for the measurement of basic magnetic properties of materials as a function of applied magnetic field and temperature. This instrument is credited to *S. Foner* [17]. The spontaneous magnetization can be determined from magnetization isotherms, according the approach of saturation law: $M = M_S\left(1-\frac{\alpha}{H}\right)+\chi_0 H$ where χ_0 is a field independent susceptibility and α is the coefficient of magnetic hardness. The magnetization measurements were performed using a commercially built *Cryogenic Free Vibrating Sample Magnetometer*, located at the "*Ioan Ursu Institute*" *– Faculty of Physics, Cluj-Napoca*. The *VSM* includes a cryostat that allows measurements in the *4 - 700 K* temperature range and fields up to *12T*, reached using conventional laboratory electromagnets and superconducting solenoids. The VSM probe and additional special set of probes to measure different material properties including magnetic moment, specific heat, Hall effect, Seebeck effect and resistivity.

4.3 Weiss balance. The horizontal Weiss balance is one of the cheapest installations, used for magnetic measurements, regarding its constructions costs, but it is very sensitive allowing the measurement of susceptibilities of 10^{-6}-10^{-7}. It can be used to perform quantitative measurements on paramagnetic and diamagnetic samples, and qualitative measurements on magnetically ordered samples. The scheme refers the installation that was constructed and functions in the *Solid State Laboratory – Faculty of Physics*, from *Babes-Bolyai University, Cluj Napoca.* The horizontal Weiss balance contains a cryostat that allows measurements in the 77-300K temperature range, and an oven for measurements in the 300-1300K temperature range. The cryostat temperature is measured with a cupper-constantan thermocouple, and in the oven with a platinum-platinum/rhodium 10% thermocouple. The molar Curie constant C is obtained from the slope of the temperature dependence of the reciprocal susceptibility at high temperatures, by linear fitting, and the magnetic moment is calculated as: $\mu_{eff} \cong 2.827\sqrt{C}$

Chapter 5. Magnetism of rare earth and 3d metals

5.1. Rare earth magnetism. Rare earths are 15 lanthanides elements from group IIIA with atomic numbers between 57 and 71 in periodic table of elements Fig1.Classification of rare earths is divided in two groups: an easy group or Cerium's group which have elements with atomic numbers between 57-63 and second group is heavy group or Yttrium's group with atomic numbers from 64 to 71. Each element is found in the earth's crust as gold silver or platinum. Rare earth is divided in two categories: easy rare earth (La-Eu more abundant) and heavy rare earth (Gd-Lu).

H																	He
Li	Be											B	C	N	O	F	Ne
Na	Mg											Al	Si	P	S	Cl	Ar
K	Ca	Sc	Ti	V	Cr	Mn	Fe	Co	Ni	Cu	Zn	Ga	Ge	As	Se	Br	Kr
Rb	Sr	Y	Zr	Nb	Mo	Tc	Ru	Rh	Pd	Ag	Cd	In	Sn	Sb	Te	I	Xe
Cs	Ba	La*	Hf	Ta	W	Re	Os	Ir	Pt	Au	Hg	Tl	Pb	Bi	Po	At	Rn
Fr	Ra	Ac^															

*	Ce	Pr	Nd	Pm	Sm	Eu	Gd	Tb	Dy	Ho	Er	Tm	Yb	Lu
^	Th	Pa	U	Np	Pu	Am	Cm	Bk	Cf	Es	Fm	Md	No	Lw

Fig.1. *The elementary table of elements*

These elements are not found in nature as free metals and the fact that minerals occurs is the result of mixture with nonmetals. Rare earths are metals which present electrical conductivity and from the chemical point of view are strong reducing agents and their compounds are generally ions. Most are trivalent compounds while europium has valence +2 and cerium has valence +4 which are the most reactive rare earths. At high temperature many of rare earths ignited and burn intensely (e.g. Eu ignited at 150-180ºC). Many rare earths are strongly paramagnetic behaviour, Ho (holmium) is one of the most paramagnetic substances. Almost all materials have magnetic characteristic to a certain temperature, others are paramagnetic or diamagnetic considered. Due to strong correlation of 4f level which is responsible for magnetic properties of rare earth they shown modest Curie temperature (293K for Gd), Nd and Sm are antiferromagnets while Eu, Er, Ho, and Tm are ferrimagnets. Rare earths have external level (5s level and 5p level) fully occupied with electrons while internal level (4f level) shows a variation of occupancy electrons (e.g. La has 0 electrons on 4f level and Lu has 14 electrons on 4f level). This electronic structure has two consequences. The first is that the external electrons give the chemical properties of rare earths and second consequence is that the internal electrons give the magnetic behavior. The magnetic effect gives by the different electrons from 4f level not cancel each other as in case of fully completed level, resulting in strong magnetization. This fact leads to use rare earths to produce permanent magnets.

5.2. Magnetism of 3d metals. Two complementary models, itinerant and localized, were used for the explication of magnetic properties of metallic systems based on 3d transition elements (Cr, Mn, Fe, Co şi Ni). Could not explain the Curie-Weiss law observed for all ferromagnetic metals for $T > T_C$. The calculated value of Curie temperature is too big comparing to the experimental one, problems that are easily resolved by localized model. The existence of a local moment at the position of 3d transition element, in pure metal, in an alloy or intermetallic compound, depend on Δ/U ratio, when $\pi\Delta/U<1$ (Anderson condition [18]), where Δ represents the width of d states (these states correspond to virtual bound states in Friedel model [19]), and U is the Coulomb correlation energy between d electrons.

One can conclude that the Anderson model explains from the theoretical point of view, in accord with experimental data and band structure calculations, the apparition probability of local magnetic moments at the position of 3d transition element. Transition elements magnetism is due to 3d electrons, which form a narrow energetic band incomplete filled. The itinerant electrons can be found in 3d and 4s bands, which are overlapped, leading to a

fractional number of d electrons responsible for the magnetic behaviour. The magnetic contribution of 4s electrons is very small and can be neglected.

5.3 Rare earth-3d transition metal intermetallic compounds.

The investigation of rare-earth (*R*) - transition metal (*M*) intermetallic compounds has been the subject of many fundamental as well as technological studies. The *R-M* intermetallic compounds are distinguished by large magnetic anisotropies, high magnetization and high *Curie* temperatures. They form an important class of materials that find applications in permanent magnets, magnetostrictive devices and magneto-optical recording.

The intrinsic properties of the *R-M* intermetallics can be understood in terms of exchange interactions and magnetocrystalline anisotropies. The exchange interactions take place between all unpaired *R*-4*f* and *M*-3*d* electrons. This interaction takes place through the hybridization of the transition metal *3d* states with the *5d* ones of the rare-earth. In *R-M* compounds it is generally accepted there are three types of interactions, namely, the *R-R* interactions between the magnetic moments within the *R* sublattice, the *M-M* interactions between magnetic moments of the *M* sublattice and the *R-M* intersublattice interactions.

The magnetic moments of R atoms and M atoms in generally depends on lattice positions. Magnetic moments of M atoms determined by neutron diffraction studies and effective magnetic moment determined by Curie constant are higher than those determined from magnetic measurements at saturation. Ratio $r = n_P/n_S$ between number of magnetic moments calculated from Curie constant and number of magnetic moments calculated from saturation magnetization give as a measure of the location of the M atoms. Accuracy localization of magnetic moment of M atoms depends by the Curie temperature.

5.4 Investigations of the materials

The spontaneous magnetization can be determined from magnetization isotherms, according the approach of saturation law: $M = M_S\left(1-\frac{\alpha}{H}\right)+\chi_0 H$. Above the Curie points, the susceptibilities, χ, were determined from their field dependences, according to Honda-Arrott plot [20], Honda-Owen [67], by extrapolating the measured values χ to $1/H\rightarrow 0$: $\chi = \chi_p + c\frac{M_s'}{H}$ were **c** is denoted a presumed magnetic ordered impurity content and M_s' is their saturation magnetization. The magnetic entropy changes were determined from magnetization isotherms, between zero field and a maximum field (H_0) using the thermodynamic relation:

$$\Delta S_m(T,H_0) = S_m(T,H_0) - S_m(T,0) = \frac{1}{\Delta T}\int_0^{H_0} M(T+\Delta T,H) - M(T,H)\, dH$$ where ΔT is

the temperature increment between measured magnetization isotherms. The magnetic cooling efficiency can be evaluated by considering the magnitude of the magnetic entropy change, ΔS_m and its full-width at half-maximum (δT_{FWHM}). The product of the ΔS_m maximum and the ($\delta T_{FWHM}=T_2-T_1$): $RCP = -\Delta S_m \times \delta T_{FWHM}$ is the so-called relative cooling power (RCP) based on the magnetic entropy change.

Chapter 6. Experimental results and discussion

Magnetic materials showing a large magnetocaloric effect (MCE) have attracted considerable attention for their potential application in magnetic refrigeration technology [7, ,21]. The compounds which undergo temperature driven paramagnetic to ferromagnetic transitions show relatively large "negative" MCE, in which the isothermal magnetic entropy change is negative [22]. Generally, due to their high magnetic moments, heavy rare earths elements and their compounds are considered as best candidate materials for finding a large MCE [23].

6.1 Structural, electronic, magnetic properties and magnetocaloric effect of $Dy_xLa_{1-x}Ni_5$ compounds

The transition metal atoms (M) in rare-earth (R) or yttrium compounds show a wide variety of magnetic behaviors. As function of crystal structure and composition, these cover the situations in which an atom show a well defined magnetism or are in nonmagnetic state, crossing the region of onset or collapse of magnetism [24]. The transition from nonmagnetic to magnetic state was analyzed mainly in cobalt compounds, by using the molecular field approximation. The RNi_5 compounds crystallize in a hexagonal structure of $CaCu_5$-type, having P6/mmm space group. The analysis of the magnetic properties of RNi_5 end series compounds evidenced interesting properties.

6.1.1 Sample preparation

The alloys $Dy_xLa_{1-x}Ni_5$ with the nominal composition x=0.5, 0.75 were prepared by high-energy ball milling technique of a mixture of high purity elements in stoichiometric proportions. The purity of the starting materials was Ni (99.99%), La (99.95%) and Dy (99.95%) delivered by the company Alfa Aesar, Jonson & Matthey, Karlsruhe, Germany. The milling was performed in a Fritsch planetary mill for 2 hours to low energy, to induce good homogeneity, followed by a high energy milling for 5h under high-purity argon atmosphere at

room temperature. It follows a good control of stoichiometry with reproducible results. In order to investigate the influence of the heat treatment on the evolution of the structural and magnetic properties, the samples of milled powder were sealed in evacuated silica tubes and heated at 1000°C for different times.

6.1.2 Structural properties of $Dy_xLa_{1-x}Ni_5$ compounds

The crystal structure of $Dy_xLa_{1-x}Ni_5$ compounds was checked by X-ray diffraction, (XRD), at the Faculty of Physics, Babes-Bolyai University. XRD was carried out with Cu K_α radiation (λ = 0.15406 nm) on a Bruker D8 X Advance diffractometer. The intensities were measured from 2θ = 20° to 100° with a step of 0.03 degree and an acquisition time of 10 seconds in order to increase measurements accuracy.

XRD patterns of the as milled $Dy_xLa_{1-x}Ni_5$ (x = 0.5, 0.75) are presented in Fig.2. The Bragg peaks corresponding to $DyNi_5$ phase are broadened by milling but no additional peaks are observed. It is known that the heat treatment is very efficient for the refinement of the structure. After milling the samples were sealed in quartz tube under vacuum and heat treated at 1000 °C for 2 hours. The X-ray diffraction patterns of the $Dy_xLa_{1-x}Ni_5$ sample milled for 5 hours and annealed at 1000 °C for 2 hours are presented in Fig.3.

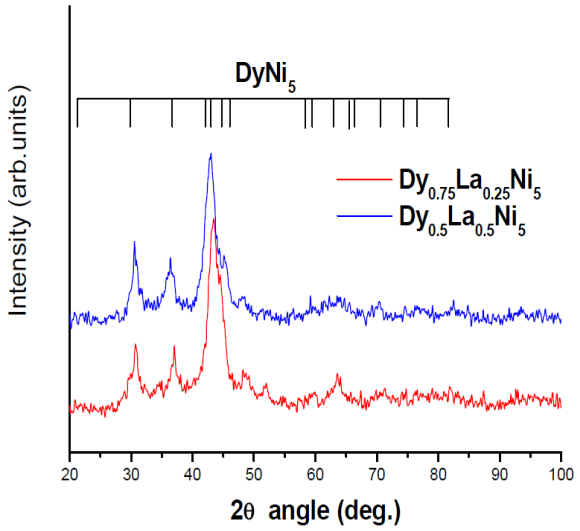

Fig..2. X-ray diffraction patterns of the $Dy_xLa_{1-x}Ni_5$ for (x= 0. 5, 0.75) milled 5 hours

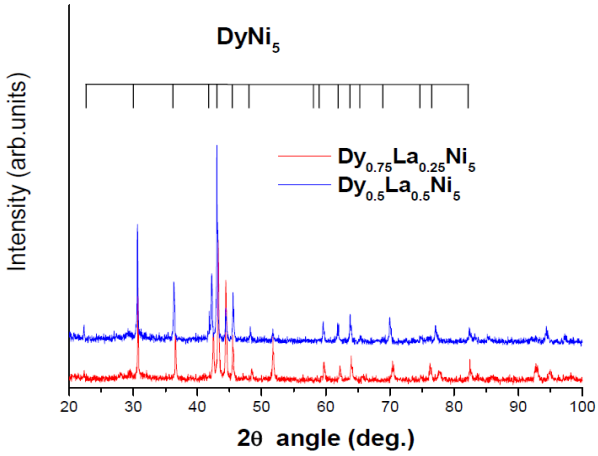

Fig.3. X-ray diffraction patterns of the $Dy_xLa_{1-x}Ni_5$ sample (x=0.5 and x=0.75) milled for 5 hours and annealed at 1000 °C for 2 hours

The sharper peaks of the X-ray diffraction patterns can be attributed to a decrease in the internal stresses. The mean size of the nanocrystallites, calculated from Full-Width-at-Half-Maximum - FWHM of the $DyNi_5$ diffraction peaks according to Scherrer's formula [25]

leads to a mean value of about 5 nm after 5 hours milling. The mean size of the nanocrystallites $Dy_xLa_{1-x}Ni_5$ (x= 0.5, 0.75) in according to Scherrer's formula [25] are around 5nm for 5 hours milling and after annealed at 1000°C for two hours the mean size of the nanocrystallites are 65nm for x=0.75 and 70nm for x=0.5.A small amount of Ni was observed for the both composition which decrease with the lanthanum concentration. From the Rietveld analysis using Fullprof software was calculated the lattice parameters, x,y,z position and occupancy.

6.1.3 Magnetic properties and magnetocaloric effect on $Dy_xLa_{1-x}Ni_5$ compounds

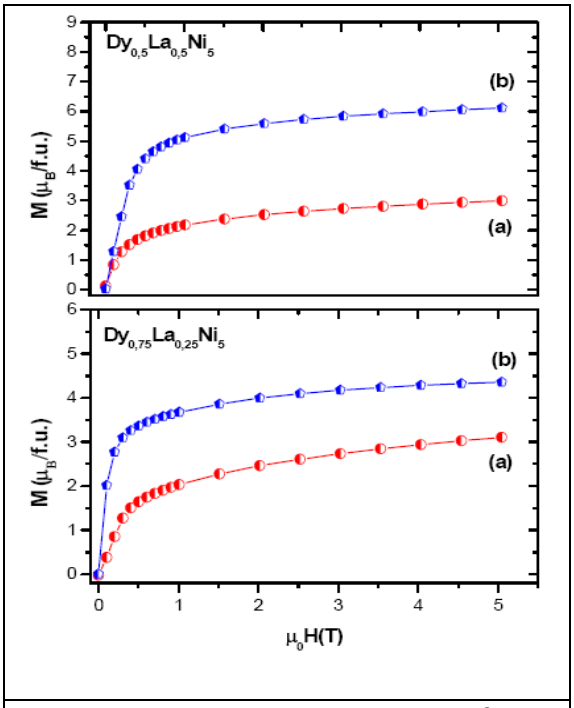

Fig. 4. Magnetization isotherms for $Dy_xLa_{1-x}Ni_5$ compounds

The magnetization curves were recorded at 4K by the extraction method in a continuous magnetic field up to 5T [26]. The saturation magnetizations M_s, were determined from magnetization isotherms, according to approach to saturation law.

Some magnetization isotherms before and after annealing are plotted in Fig.4. There are high differences between the magnetizations, the values for the samples as milled being smaller with around $3\mu_B$ for x=0.5 compound compared with the values obtained for the annealed sample. This high difference can be explained by the presence of Dy_3Ni and unreacted Ni in the milled sample as was shown by the Rietveld analysis. The total calculated amount of Dy_3Ni is around 10%.

By this method any possible alteration of magnetic susceptibilities, as result of the presence of magnetic ordered phase, is avoided. Generally, no magnetic ordered phases, above T_c, were observed. Even when exist, these are smaller than 0.1 mol %. Some magnetization isotherms in external

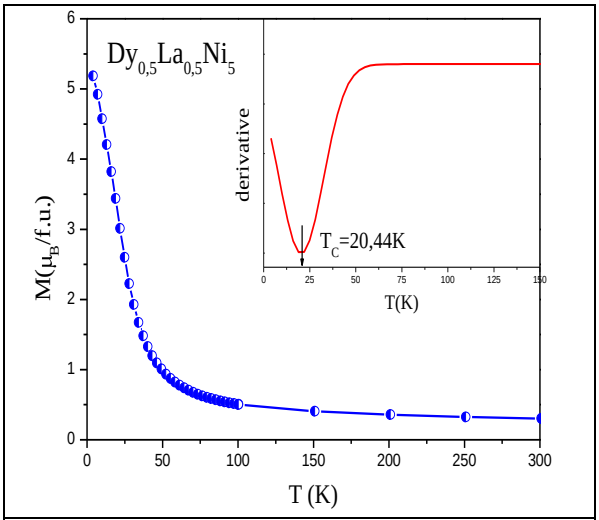

Fig.5.Temperature dependences of magnetisation for $Dy_{0.5}La_{0.5}Ni_5$

magnetic fields up to 3 T, after annealing are plotted in Fig.6. One can see that the saturation is not attended in this field. A transition from an ordered state to a paramagnetic behavior could be clearly seen too.

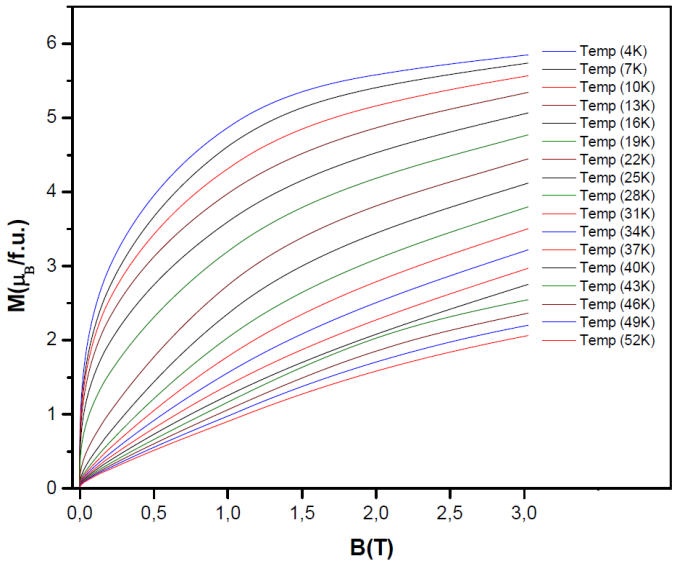

Fig.6. Magnetization isotherms taken around transition temperature for the annealing compound with x=0.75

In the case of the $Dy_{0.5}La_{0.5}Ni_5$ sample, the transition temperatures can easily be observed in Fig.5. The transition temperature was determinate by the numerical dM/dT derivative and a value of 20.44K was obtained for the transition temperature (T_C) in a magnetic field of $\mu_0 H$=0,2T.

The magnetic entropy changes were determined from magnetization isotherms, Fig.6 between zero field and a maximum field (H_0) using the thermodynamic relation (6.2) with an increment in temperature between measured magnetization isotherms (ΔT = 3K for our data). A maximum value of of 5.6 J/(kgK) was obtained for a variation of the external magnetic field between 0 and 3 T.

The temperature dependence of the magnetic entropy change for the sample with x=0.75 is presented in Fig. 7. One can see that the curves are quite symmetric distributed around the transition temperature. This behavior is generally characteristic for a second order phase transition.

The magnetic cooling efficiency was evaluated by considering the maximum value of the magnetic entropy change, ΔS_m and its full-

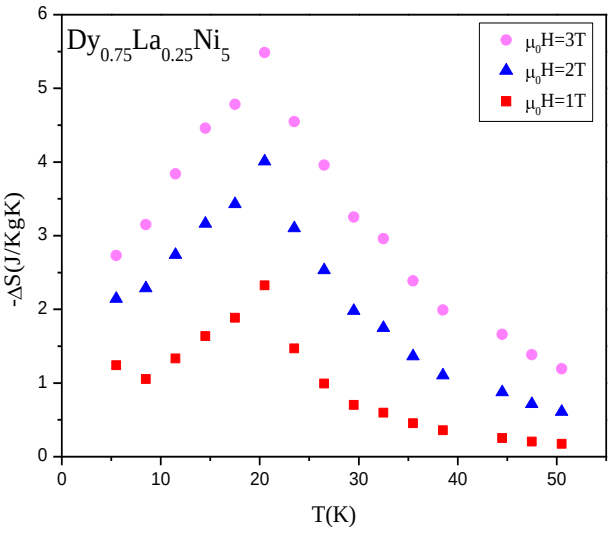

Fig.6.7. Magnetic entropy changes around transition temperature for the annealed compound with x=0.75.

width at half-maximum (δT_{FWHM}). The product of the ΔS_m maximum and the ($\delta T_{FWHM}=T_2-T_1$) is the so-called relative cooling power (RCP) based on the magnetic entropy change.

In the case of samples with lower Dy content the -ΔS values have smaller values. Values between 146 J/kg (in 3T) and 21 J/kg (in 1T) of the RCP(S) were determined.

6.1.4 Band structure calculation results

In order to a better understanding of the physical properties of these compound we have performed band structure calculations Fig.8. Band structure calculations were carried out by using the LSDA+U method. The LSDA+U [27] scheme, introduces a simple mean-field Hubbard like term to the LSDA functional. This approach can be viewed as a density functional approach since the U term depends on the occupation number for localized electrons and is determined by the total density. In the actual calculations we have used for the averaged local Coulomb interaction the value U=6 and the exchange parameter J=0.9. Dy_3Ni_{15} superstructure having three times greater unit cell than that of $DyNi_5$ was assumed. In this cell, the Dy was substituted by one, two or three lanthanum atoms, corresponding to compositions x = 0.67, 0.33 and 0.

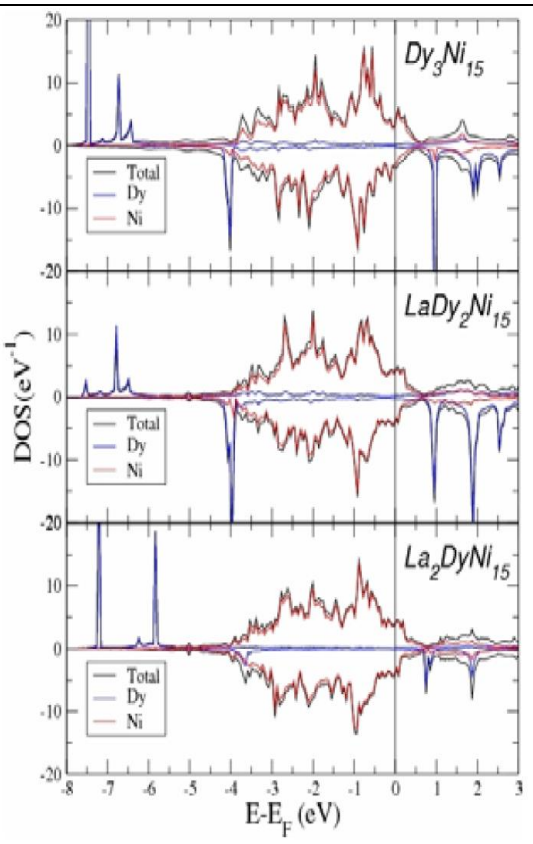

Fig.8. Dy_3Ni_{15}, Dy_2LaNi_{15} and $DyLa_2Ni_{15}$ densities of states

The total densities of states, (DOS), as well as the partial DOS for Ni and Dy projected bands for $Dy_xLa_{1-x}Ni_5$ compounds with x = 1.0; 0.67 and 0.33 are plotted in Fig.6.8.

The strength of exchange interactions between nickel atoms and dysprosium ones are more important than between nickel atoms. The nickel moments are essentially induced by the exchange interactions due to presence of Dy. Thus, the exchange splitting of Ni(2c) 3d band is greater than for Ni(3g) sites since of the higher number of Dy nearest neighbours. The La substitution by Dy, leads to the variations of the exchange interactions and consequently to different exchange splitting of Ni3d bands when increasing dysprosium content.

The magnetic behaviour of nickel in RNi5-based compounds can be analyzed in models which take into account the electron correlation effects in d-band, as spin fluctuation model [28] or dynamical mean field theory [29]. The above models reconcile the dual character of electron, which a particle, requires a real space description and as a wave, a momentum space description. According to the last model, for an itinerant electron system, the time dependence of the correlation function results in a temperature dependence of fluctuating moments.Fluctuating moments and atomic like configurations are large at short time scale. The moments are reduced at larger time scale. In spin fluctuation model [28] the balance between longitudinal and transverse spin fluctuations is considered. This leads to the concept of temperature induced moments, when the frequency of transverse spin fluctuations are higher than of the longitudinal ones.

6.1.5 Preliminary conclusions

Sample was milled at low energy to induce good homogeneity, followed by a high energy milling using the Fritch planetary mill.. This technique follows a good control of stoichiometry with reproducible results. In order to obtain good result the samples of milled powder was heated at 1000°C for different times.

In $Dy_xLa_{1-x}Ni_5$, system there is a transition from spin fluctuations behaviour, characteristic for $LaNi_5$, to a ferrimagnetic type ordering for $x \geq 0.2$. The 4f–3d exchange interactions are mediated by R5d band. The Dy5d band polarization is due both to local 4f–5d exchange and 5d–3d and 5d–5d band hybridizations by short range exchange interactions with neighbouring atoms. The mean effective nickel moments decrease when increasing dysprosium. The magnetic behaviour of nickel can be described in the spin fluctuation model. The magnetic entropy change have maximum values around 6J/(kgK) in a 3T external magnetic field [30]. The relative cooling power (RCP) has enough high values to could consider this system for technical applications.

6.2. Structural and magnetic properties of $Tb_8Co_{16-x}Cu_x$ compounds

To investigate magnetocaloric effect several Laves phase compounds have been studied because they present a simply crystal structure [31-33]. The RCo_2 intermetallic compounds (R= rare earth metal) were intensively studied due to the metamagnetic character of its cobalt sublattice [34,35]. When R is nonmagnetic there are necessary high fields (> 70T in YCo_2) in order to induce magnetic moments on cobalt atoms and giving rise to

metamagnetic transitions. If R is a magnetic atom the internal field is high enough to induce and polarize the cobalt moments.

The RCo_2 compounds crystallize in a cubic Laves phase structure of C15 type . The prototype compound for this structure is $MgCu_2$. Because of the high symmetry of this lattice, the study of these compounds may give useful information on the magnetic behavior of the constituent atoms [36,37]. The $TbCo_2$ compound was reported to be ferrimagnetically ordered. In the paramagnetic region a non-linear temperature dependence of the reciprocal susceptibility was reported. In order to obtain additional information on transition metals behavior in pseudobinary compounds we study the magnetic properties of cobalt in $Tb_8Co_{16-x}Cu_x$ system in the range with rich cobalt content. In all cases the magnetic entropy changes around transition temperatures were evaluated.

6.2.1. Sample preparation

The $Tb_8Co_{16-x}Cu_x$ compounds were prepared by arc melting in a purified argon atmosphere from high purity Co (99.9%), Cu (99.999%) and Tb (99.95%) ingots delivered by the company Alfa Aesar, Jonson & Matthey, Karlsruhe, Germany). A small excess of rare earth element was used in order to compensate for losses during melting. The ingots were remelted several times in order to ensure a good homogeneity. The samples were sealed in quartz tube in vacuum and heat treated at 1000 ºC for 5 days.

6.2.2. Structural characterization of $Tb_8Co_{14}Cu_2$

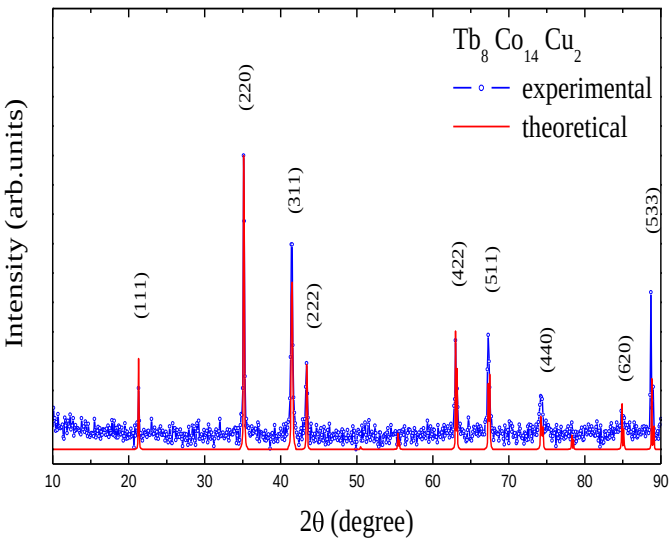

Fig.9. X-ray diffraction patterns of the $Tb_8Co_{14}Cu_2$ sample

The crystal structure was checked by X-ray Diffraction using a Bruker 8 XD diffractometer at the Faculty of Physics, Babes – Bolyai University. XRD was carried out with Cu K_α radiation (λ = 0.15406 nm) at room temperature measured in 2θ = 10° to 90° with a step of 0.1 degree and an acquisition time of 10 seconds in order to increase measurements accuracy . As example the X-ray

diffraction patterns of the $Tb_8Co_{14}Cu_2$ sample are presented in Fig.9. Similar results were obtained in all cases. The X-ray analysis shows, in the limit of experimental errors, the presence of one phase only, for $x \leq 4$, of C15 type. The lattice parameters decrease slightly when Cu content increases, fact attributed to smaller radius of Cu ion compared with Co one. The analysis of diffraction pattern was investigated using the PowderCell software.

6.2.3. Magnetic properties and magnetocaloric effect in $Tb_8Co_{16-x}Cu_x$

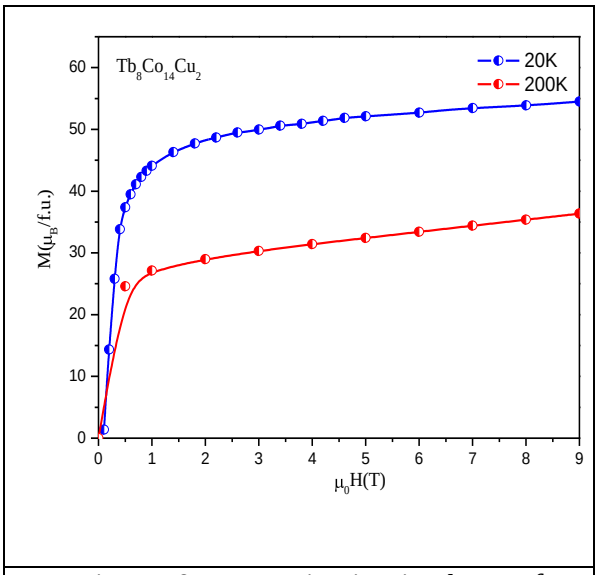

Fig. 6.10. Magnetization isotherms for $Tb_8Co_{14}Cu_2$ compound

The magnetic measurements were performed in the temperature range 4.2-650K and external fields up to 12T using a Vibrating Sample Magnetometer (VSM) from Cryogenics

In Fig.6.10 are presented two magnetization isotherms for different temperature. Blue line represent the magnetic isotherm at 20K in a magnetic field up to 12T and red line shows magnetization isotherm at 200K in the same range of magnetic field. From these curves it can be obtain the saturation magnetization at different temperatures in a temperature range from 20K to 275K. The magnetization

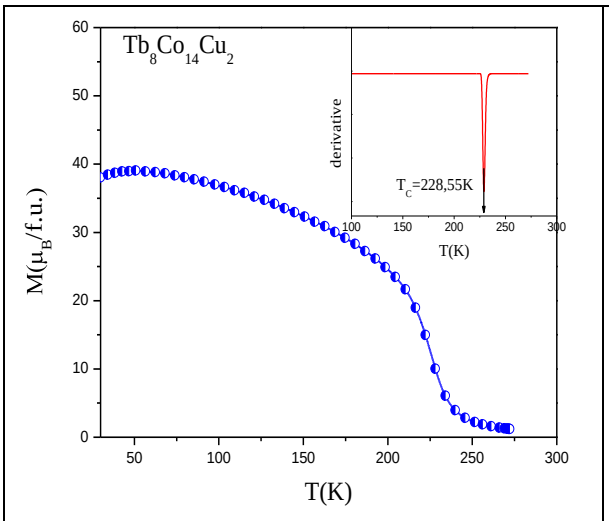

Fig.11.Temperature dependences of magnetisation for $Tb_8Co_{14}Cu_2$

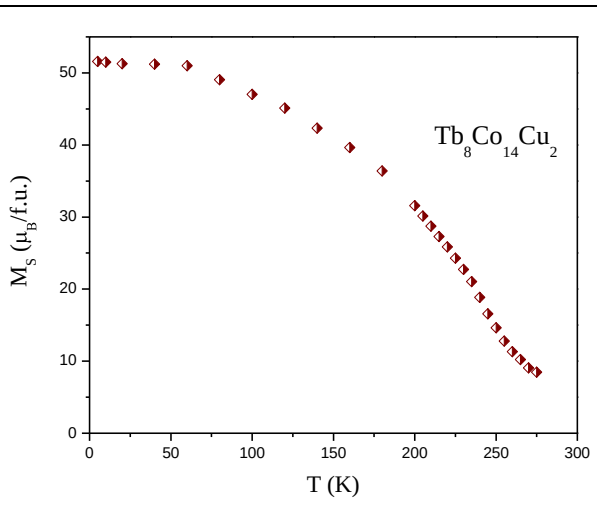

Fig.12. Spontaneous magnetization for $Tb_8Co_{14}Cu_2$ compound

isotherms measured in magnetic fields up to 12 T shows that the saturation is not attended. In the case of the $Tb_8Co_{14}Cu_2$ sample, the transition temperatures can easily be observed .

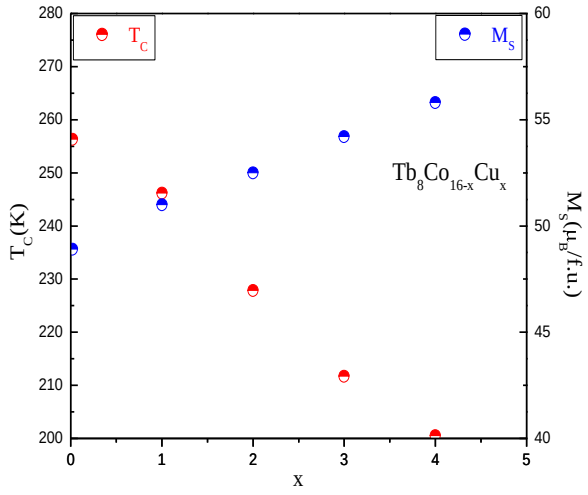

Fig.13. The composition dependences of the Curie temperatures and spontaneous magnetizations measured at 4.2 K.

The transition temperature was determinate by the numerical dM/dT derivative and a value of 228.55K was obtained for the transition temperature (T_C) in a magnetic field of μ_0H=0,5T Fig.11. The saturation is not attended even in 9T magnetic external fields. Similar behaviors were obtained in all cases. The spontaneous magnetizations, M_s, were determined from magnetization isotherms. The magnetizations, at 4.2 K, increase from 48.96 μ_B/f.u. at x = 0 to 55.76 μ_B/f.u. at x = 4 –see Fig.13. The above behavior is in agreement with the presence of a ferrimagnetic type ordering, the cobalt and terbium magnetic moments being antiparallely oriented.

Assuming that the terbium mean magnetic moment, at 4.2 K, is the same like that determined on $TbCo_2$ compound by neutron diffraction study [104] the cobalt contributions to magnetizations were determined. The cobalt moments are little dependent on Cu content having values in the range 1.1±0.09 μ_B/atom Fig.14. The Curie temperatures decrease when copper content increase – Fig.6.15.The Curie constants, determined in the above temperature ranges, are higher than the characteristic values for Tb^{3+} ion suggesting the presence of contributions from the cobalt atoms. According to addition law of susceptibilities and supposing that the Curie constant of terbium is the same as that of Tb^{3+} ion, we determined the contributions of Co, to the Curie

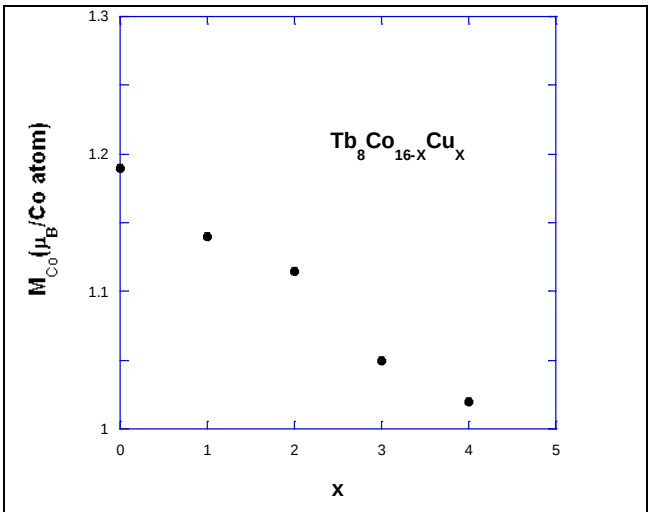

Fig.14. The cobalt moment dependence on Cu content

constants and the effective cobalt moments, M_{eff}(Co), respectively. The M_{eff}(Co) values are only slightly composition dependent being 2.81±0.12 μ_B/atom.

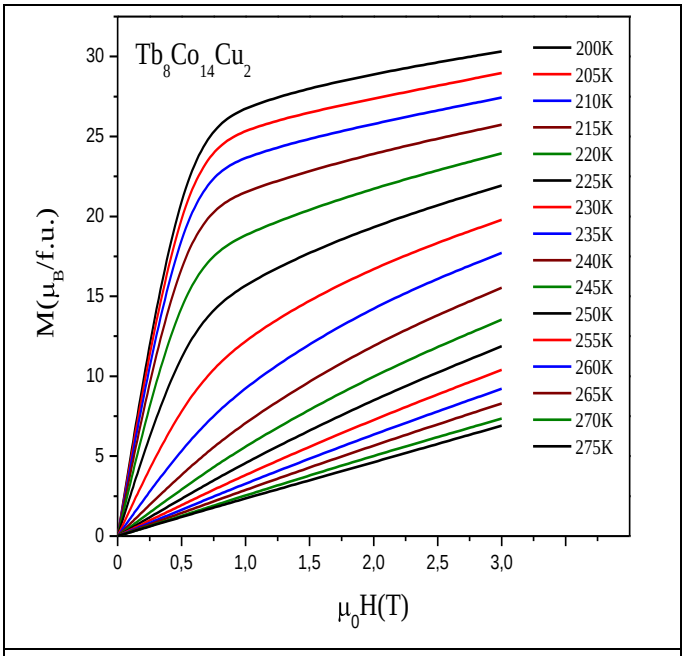

Fig.15. Magnetization isotherms taken around transition temperature

The temperature dependences of reciprocal susceptibilities, χ^{-1}, follow a hyperbolic law of Néel- type, characteristic for ferrimagnetic ordering. At high temperatures, the χ^{-1} vs. T plots shows linear dependences.

The ratio $r=S_P/S_0$ between the number of spins obtained from effective cobalt moments, S_P, and saturation moments, S_0, is quite constant having values around 1.73±0.07. In the local moment limit we have r=1.0. For a weak ferromagnet the r values increase considerably. In our compounds the r value suggests that cobalt have rather high degree of itinerancy. The above behaviour can be analyzed in spin fluctuation model [28,38].

The magnetization isotherms in magnetic fields up to 3T around the transition temperature for the $Tb_8Co_{14}Cu_2$ compound are presented in Fig.15. with an increment between measured magnetization isotherms $\Delta T = 5K$ for our data. The magnetic entropy changes were determined from magnetization isotherms, Fig.16. between zero field and a maximum field (H_0) using the thermodynamic relation (5.2) with an increment in temperature between measured magnetization isotherms (ΔT = 5K for our data). The maximum values of entropy change occur almost at the Curie temperature. The maximum value is around 4.15J/kgK in a 3T respectively 3 J/kgK in 2T external magnetic field for the compound with x = 2 Fig 6.19. The relative cooling power has enough high values to could

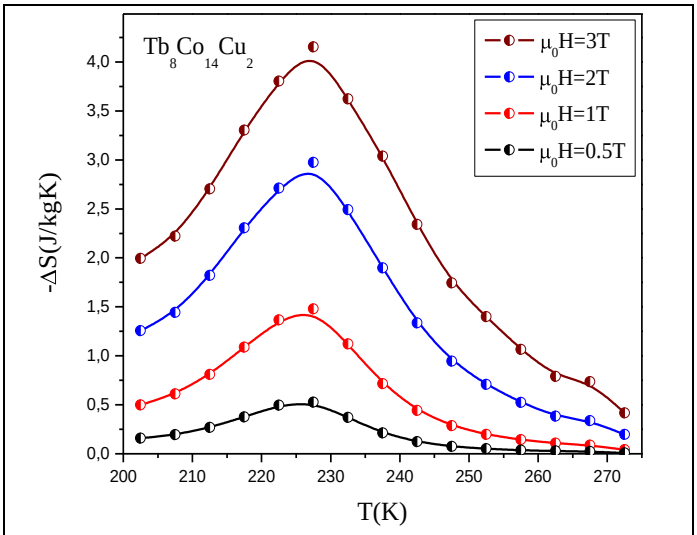

Fig.16. Magnetic entropy changes around transition temperature for $Tb_8Co_{14}Cu_2$ compound

consider this system for technical applications. A large RCP(ΔS) corresponds to a better magnetocaloric material.

6.2.4. Preliminary conclusions

We have studied the magnetic properties and the magnetocaloric effect in $Tb_8Co_{16-X}Cu_X$ compounds with Laves phase structure. The cobalt behavior in these compounds can be described as a weak ferromagnet. Partial quenching of spin fluctuation by internal field was observed. Large magnetic entropy changes have been observed for all concentrations. The transition temperature can be tuned via Cu concentration. These suggest that $Tb_8Co_{16-X}Cu_X$ has a potential application as a working substance of magnetic refrigeration in the temperature range 190K-270K [39,40].

6.3. Electronic structure and magnetocaloric effect in $Tb_{8-x}Y_xCo_{16}$ compounds

Magnetic

Generally, due to their high magnetic moments, heavy rare earths elements and their compounds are considered as best candidate materials for finding a large MCE [41].

Because of the high symmetry of this lattice, the study of these compounds may give useful information on the magnetic behavior of the constituent atoms [37,42]. Voiron et al. [43] have measured specific heat in $TbCo_2$ at zero applied field, and no anomalous behavior was found above Tc: It was reported that the substitution of magnetic R-atom by yttrium reveals a decrease of the magnetic order and finally leads to an exchange-enhanced Pauli paramagnetism in YCo_2. The composition dependence of Co-magnetic moment in the $R_{1-X}Y_XCo_2$ systems shows a sharp fall approaching a critical yttrium concentration x_c. Previously, studies of the behavior of rare earth and Co magnetic subsystems with Y-substitution were performed for the $R_{1-X}Y_XCo_2$ compounds with R= heavy rare earths[44-51]. The magnetic state of $Tb_{1-X}Y_XCo_2$ is different in two concentration ranges. The concentration range $0 < x < 0.8$ corresponds to the ferromagnetic order while in the second concentration range $0.8 < x < 1.0$ the compounds become paramagnetic [48]. The RCo_2 compounds were R is a heavy rare earth are ferrimagnetically ordered, the R magnetization being antiparallel oriented to that of cobalt. The magnetic properties of these compounds can be analysed by considering a two sublattice model. Previously, we have studied the magnetic properties in $TbCo_{2-X}Cu_X$ compounds. It was shown that the cobalt magnetic moment is sensitive to the local environment. In order to obtain additional information on transition metals behavior in pseudobinary compounds we study the electronic properties and the magnetocaloric effect in

$Tb_{8-X}Y_X$ Co_{16} system in the range with x=1,2,3,4,5,and 6. In all cases the magnetic entropy changes around transition temperatures were evaluated.

6.3.1. Structural properties of $Tb_{8-X}Y_XCo_{16}$ compounds

The $Tb_{8-X}Y_XCo_{16}$ compounds were prepared by arc melting of the constituent elements in a purified argon atmosphere from high purity Co (99.9%), Y (99.99%) and Tb (99.95%) ingots (Alfa Aesar, Jonson & Matthey, Karlsruhe, Germany). A small excess of rare earth elements was used in order to compensate for losses during melting. The ingots were remelted several times in order to ensure a good homogeneity. The samples were heat treated in vacuum at 950 ºC for 5 days. The crystal structure was checked by X-ray Diffraction using a Bruker 8 XD diffractometer. Structure refinement was performed according to the Rietveld technique, supported by the FULLPROF computer code [52].

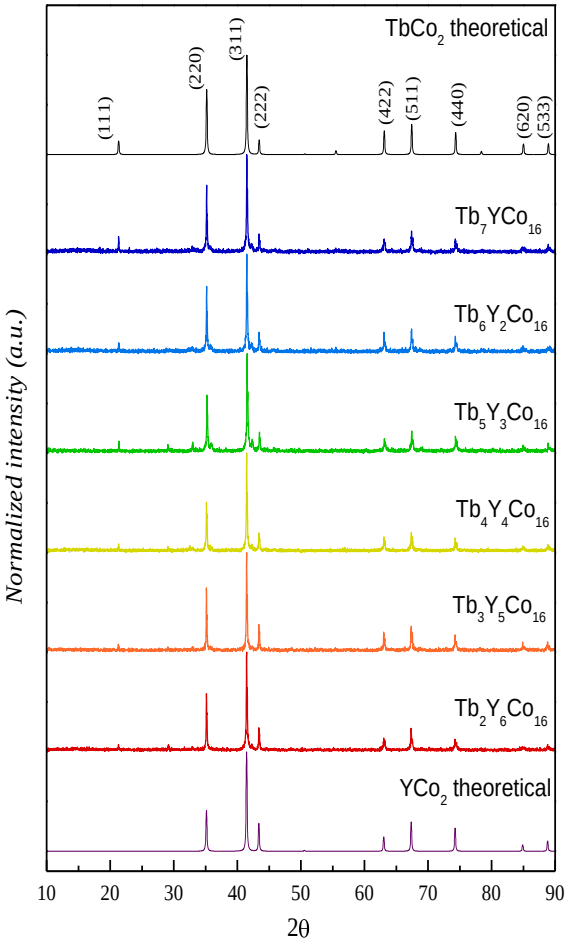

Fig6.20. Diffraction patterns of $Tb_{8-X}Y_X$ Co_{16} compounds

The X-ray analysis shows, in the limit of experimental errors, the presence of one phase only, for $x \leq 6$, with the cubic $MnCu_2$ structure Fig.17.

6.3.2. Electronic structure of $Tb_{1-X}Y_XCo_2$ compounds

The electronic structure of the $Tb_xY_{1-x}Co_2$ compounds has been calculated self-consistently by means of the spin polarized relativistic Korringa- Kohn-Rostocker (SPR-KKR) method in the atomic sphere approximation (ASA) mode [53]. The calculation method is based on the KKR-Green's function formalism that makes use of multiple scattering theory. Exchange and correlation effects have been treated within the framework of the local density approximation, using the parameterization of Vosko et al. [54].

The projected total density of states for the compound $Tb_{0.25}Y_{0.75}Co_2$ compound and for Co are plotted in Fig.18. while in Fig.19. are presented the partial density of states for Tb respectively Y in $Tb_{0.25}Y_{0.75}Co_2$ compound. One can see that the Fermi level is situated above the characteristic double sharp peak structure of local DOS of cobalt d states. The double peak structure of Co d states is little affected in intensity, when Y content increases, more important changes being evidenced for the peak situated near Fermi level. The yttrium contribution to the total density of states at the Fermi level is little, a small magnetic moment being induced on the Y site by the presence of Tb atoms in the neighborhood.

a)

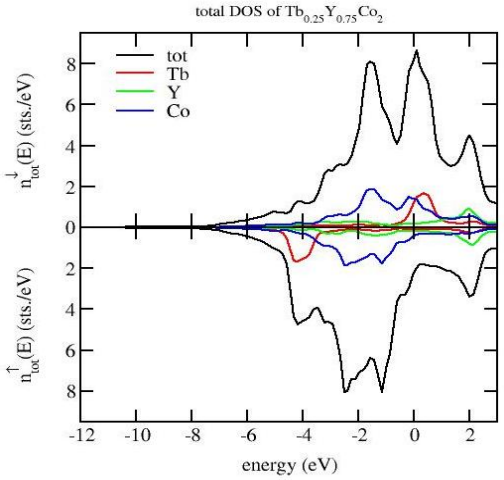

b)

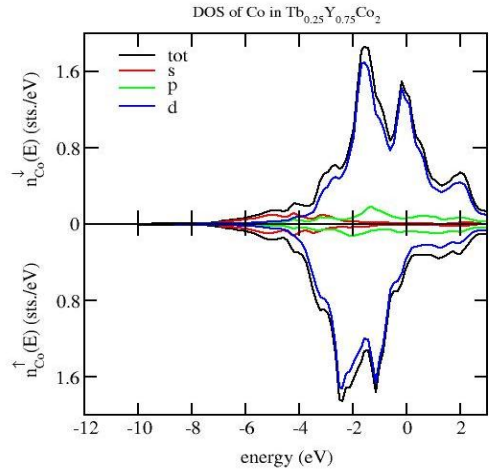

Fig.18. Projected total density of states calculated for the compound $Tb_{0.25}Y_{0.75}Co_2$

Fig. 19. Projected total density of states of for Co calculated in the compound $Tb_{0.25}Y_{0.75}Co_2$

The total state density at the Fermi level decreases slightly when the yttrium content increase. The exchange coupling between R and M electron spins is indirect. The band structure calculations and magnetic measurements performed on RM_2 [30,55] compounds suggested that there is an interplay between induced R 5*d* band polarizations and M 3*d* magnetic moments. The M 3*d* magnetic moments are influenced by the R 5*d* band polarizations. This will contribute additionally to M 3*d* polarization. The R 5*d* band polarizations, induced by short range exchange interactions, are dependent, in a first approximation, on the number of magnetic M atoms situated in the first coordination shell and their moments.The origin of the ferromagnetic state is the difference between the 3d-5d (4d) mixing in the majority and minority spin bands. As a consequence a magnetic moment on Y site appears. The changes in the neighborhood of the Co atoms through substitution of Y for Tb will modify the

contribution associated with R 5*d*–M 3*d* hybridization and finally the cobalt magnetic moment.

6.3.3. Magnetic properties and magnetocaloric effect of $Tb_{1-X}Y_XCo_2$ compounds

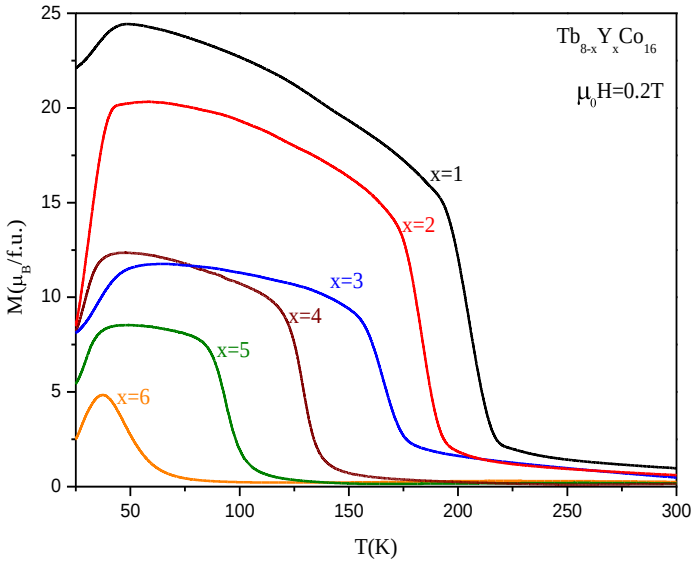

Fig.20. The temperature dependences of magnetizations measured in low magnetic field of 0.2 T.

The temperature dependences of the magnetization measured in a low magnetic field of 0.2 T are presented in Fig.20. The transition temperature decreases when terbium atoms are replaced by yttrium ones. The Curie temperatures were defined as the temperatures at which the *dM/dT* versus temperature curves measured during heating present a minimum.

The T_C values were found to decrease approximately linearly with increasing Y content in the composition region $0 \leq x \leq 3$ –see Fig.21. This decrease becomes more rapid for $x > 3$. The decrease in transition temperature, T_C, can be attributed to the fact that the Co-Co exchange interactions become weaker when terbium content decrease. This assumption is sustain by the magnetic moments of Co which decrease with increasing yttrium content. The nonlinear decrease of the transition temperatures can be attributed to the different f-d exchange interaction with increasing yttrium concentration. Similar behavior was reported in the past in $(ErY)Co_2$ [56] respectively $(GdTb)Co_2$ compounds [56].The magnetization isotherms, measured in external applied magnetic fields up to 12 T, are presented in Fig.22. The

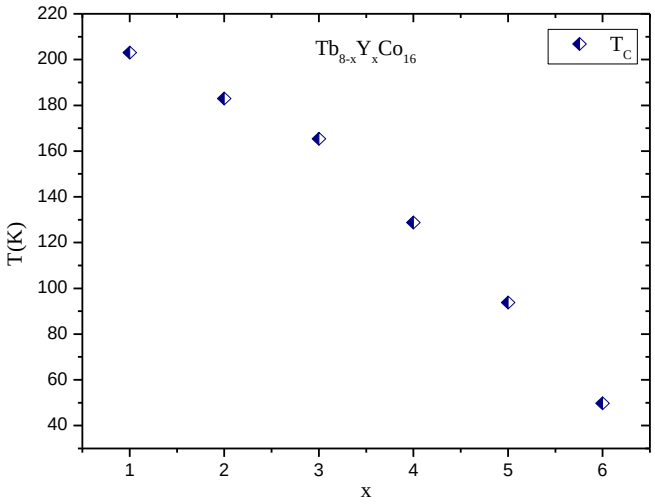

Fig.21. *The composition dependences of the Curie temperatures for the $Tb_{1-X}Y_XCo_{16}$ compounds .*

investigated compounds are ferrimagnetically ordered, the Tb and Co moments being antiparalelly oriented. The saturation moments at 5 K were determined by using the approach to saturation law, by fitting the magnetization isotherms using relation (4.2).

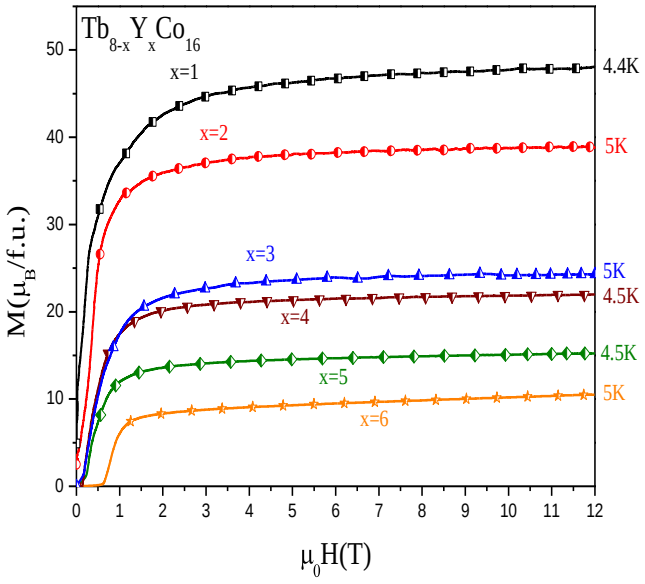

Fig.22. The magnetization isotherms measured in external magnetic fields up to 12 T.

The magnetization isotherms for the sample with x = 1 measured in a wide temperature range around the transition temperature with a step of 5 K are shown in Fig.23. From the magnetization isotherms we have calculated and represent in Fig.24. the Arrott plots [57]. The order of the magnetic transition can be derived from the shape of the M^2 versus H/M dependences. The negative slope or inflexion point on Arrott plots are usually indicative of a first-order transition, while the linear shape of thesedependencies above T_C implies that a second-order magnetic transition occurs. From the Arrot plots, we can see that the compounds undergo a second-order magnetic phase transition at the Curie temperature even if the transition is not pure.

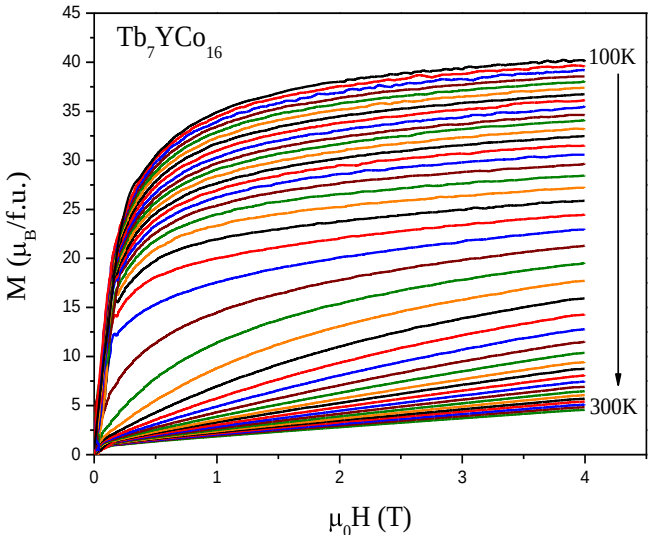

Fig.23. Magnetization isotherms for the Tb_7YCo_{16} compounds

The magnetocaloric effect in external magnetic fields between 0 and 4 T was also studied. The magnetic entropy change was calculated from magnetization isotherms using the Maxwell relation. Fig.25. shows the magnetic entropy change as a function of temperature for different magnetic field changes for the compounds with x = 1 and x=6. The ΔS_M (T) peaks are broad and have a symmetrical

shape around the transition temperature for the samples with high terbium content, a behavior which is characteristic for materials exhibiting a second-order magnetic phase transition [58].

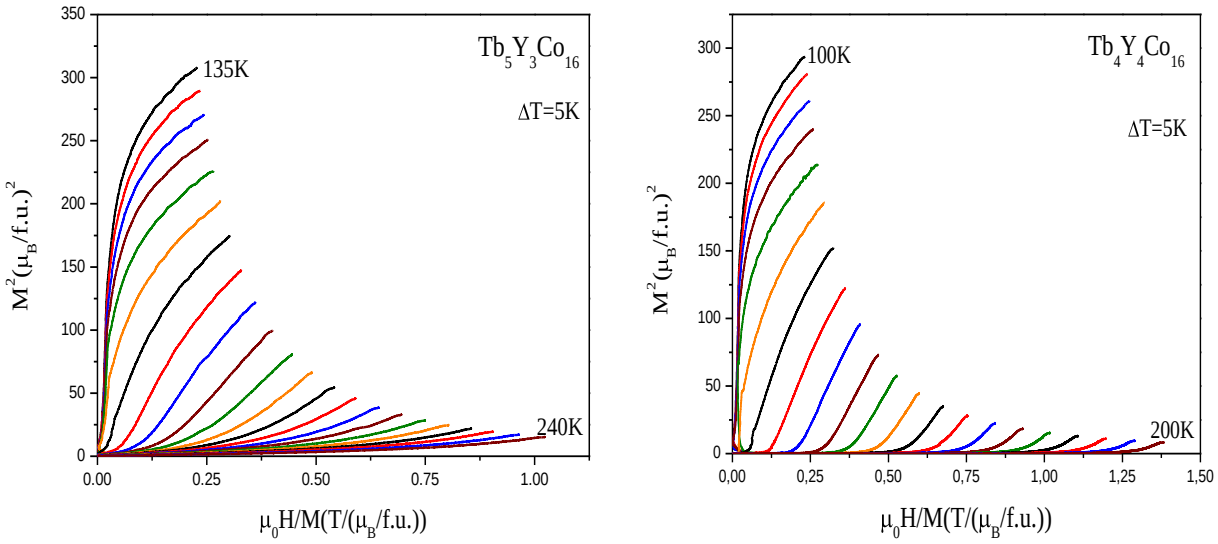

Fig.24. Arrott plots for the $Tb_{1-X}Y_XCo_{16}$ compounds with x=3 and 4.

In the case of compounds with high yttrium content the shape of the ΔS_M (T) peaks are only approximately symmetric fact that suggest that the magnetic transition is not purely of

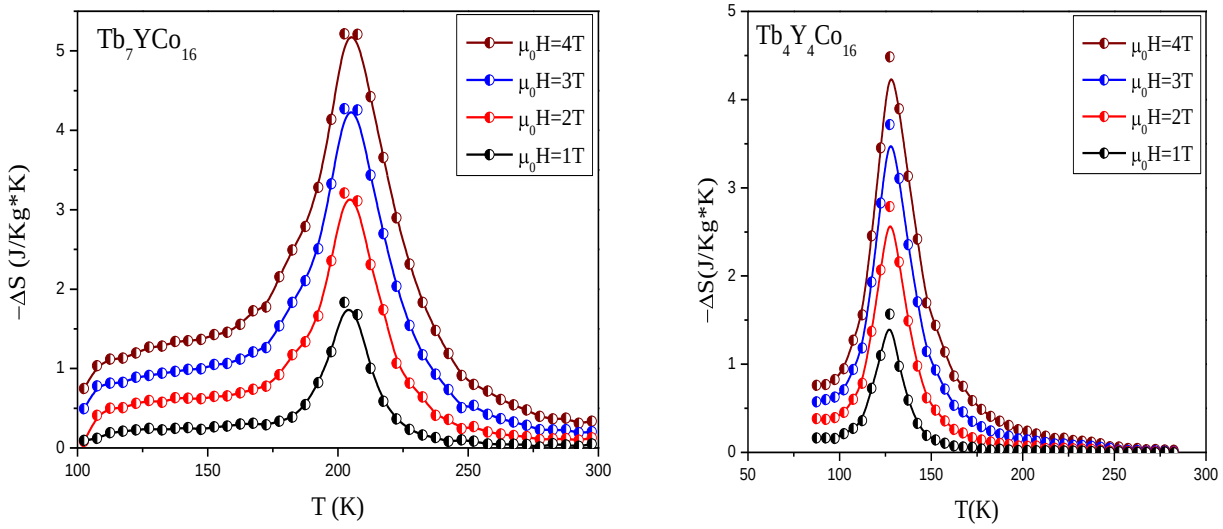

Fig.25. The magnetic entropy changes as function of temperature in different external magnetic fields for the $Tb_{1-X}Y_XCo_{16}$ compounds with x=1 and 6

second-order. The obtained maximum entropy change values were found to decrease from 5.3 J/kgK for x = 1 to 1.9 J/kgK for x = 6 for a magnetic field change from 0 to 4 T. In an external magnetic field change from 0 to 2 T, the magnetic entropy change values were found to decrease to 3.25 J/kgK for x = 1 and 1.2 J/kgK for x = 6 respectively. The decrease of magnetic entropy change with increasing yttrium content may be caused by the decrease in the concentration of Tb^{3+} ions.

The magnetic entropy change versus temperature plots in applied field changes of 0-2 T and 0-4 T for all of the investigated compounds are presented in Fig.26.

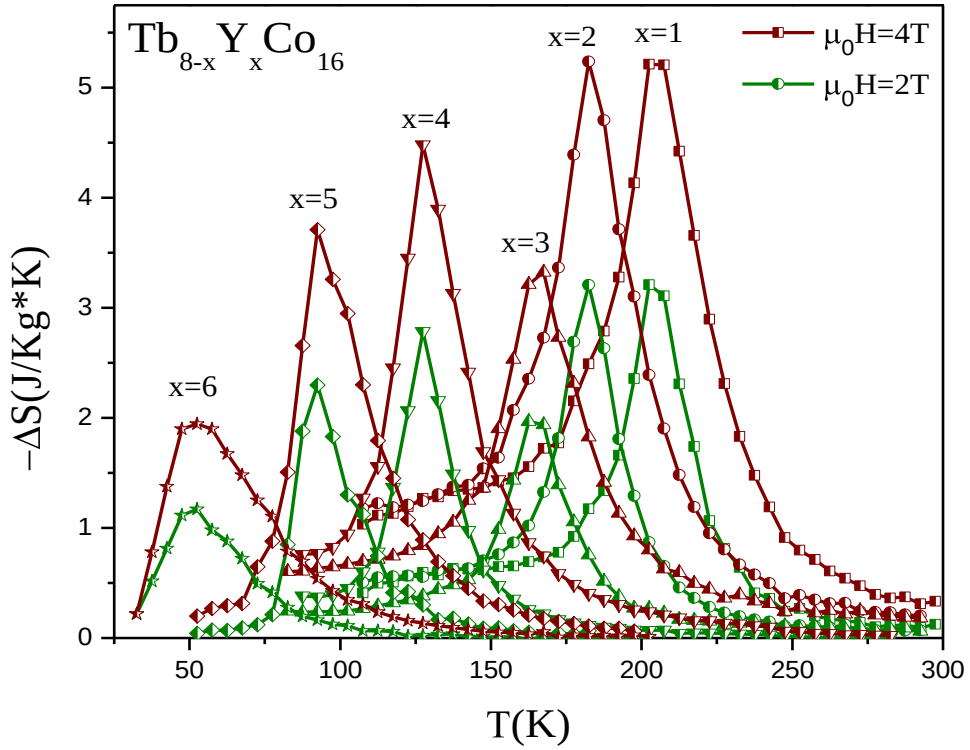

Fig.26. The magnetic entropy changes as function of temperature in applied field changes of 0-4 T and 0-2 T for all of the investigated samples belonging to the $Tb_{1-X}Y_XCo_2$ system

A characteristic parameter for magnetocaloric materials is the relative cooling power (*RCP*). A large *RCP*(*ΔS*) corresponds to a better magnetocaloric material. Also, it is worthwhile to note that the *RCP*(*ΔS*)/*ΔB* values do not vary significantly for applied field changes of 0-4 T and 0-2 T respectively, a fact which is important for magnetic refrigeration applications in the intermediate temperature range.

6.3.4. Preliminary conclusions In this research, the structural, magnetic and magnetocaloric properties of $Tb_{1-X}Y_XCo_2$ compounds were presented. Some general structural and magnetic properties have been considered for the RM_2 class of intermetallic compounds.

The $Tb_{1-X}Y_XCo_2$ compounds.with x = 1,2,3,4,5 and 6 were successfully prepared. X-ray diffraction measurements confirm the formation of the cubic $MgCu_2$ (C15) structure in all of the investigated samples. The lattice parameters were found to be little dependent on yttrium content. All of the investigated compounds were found to be ferrimagnetically ordered. The cobalt magnetic moments at 4.2 K were found to decrease with increasing Ycontent. The Curie temperature was found to decrease with increasing Y content. There are local 4f–5d exchange interactions as well as 5d–3d short range interactions with neighboring Co atoms to the Tb one. The variations of cobalt moments, when substituting magnetic Tb by nonmagnetic Y, can be attributed to diminution of the exchange interactions.

The magnetocaloric effect was also studied. The obtained maximum entropy change values were found to decrease from 5.3 J/kgK for x = 1 to 1.9 J/kgK for x = 6 for a magnetic field change from 0 to 4 T. In an external magnetic field change from 0 to 2 T, the magnetic entropy change values were found to decrease to 3.25 J/kgK for x = 1 and 1.2 J/kgK for x = 6 respectively. The decrease of magnetic entropy change with increasing yttrium content may be caused by the decrease in the concentration of Tb^{3+} ions. The large *RCP* values obtained in these materials were mainly attributed to the large δT_{FWHM} values. It was found that $RCP(\Delta S)/\Delta B$ values are quite independent of Yconcentration. Due to their high *RCP* values these compounds are promising candidates for applications in magnetic refrigeration devices in the intermediate temperature range.

6.4. Perovskite characterization

Physical properties of such perovskite systems based on manganese are dictated mainly by manganese ions whose valence can be changed from 3^+ to 4^+. Manganese 3^+ ions have $t_{2g}^3e^1$ configuration and manganese 4^+ ions have t_{2g}^3 configuration. In perovskite system based on manganese electron e_g coupled with electron t_{2g} in a feromagnetic model. This coupling leads to a ferromagnetic interaction between electrons. This process is known as the double exchange. Perovskite systems are characterized by the general formula ABO_3 were A positions are occupied by the ions of rare earth and B positions are occupied by the ions of 3d transition metal. The perovskite class presents a $CaTiO_3$ type structure. For a long time period was thought to be a perfect cubic structure. After some investigation it was noticed that shows distortions. Another effect observed in perovskites based on manganese is magnetoresistance. This is an intrinsic phenomenon which has a big value around the Curie temperature. The energy from an external magnetic field is comparable with energy of

thermal agitation and energy of double change mechanism. At low temperature below Curie temperature, some perovskites present a ferromagneticaly ordered. When a external magnetic field is applied the resistivity become very small. Refrigeration in the temperature range 250K–300K is of particular interest due to the potential impact on energy savings and environmental concerns. The interplay between structure, magnetic and transport properties in perovskite-type manganites was the aim of many recent papers.

6.4.1. Structural and magnetic properties of perovskite compounds $La_{2/3}Sr_{1/3}Mn_{1-x}Co_xO_3$

The substitution of the trivalent element by a divalent one produces an inhomogeneous distribution of mixed valence Mn^{4+}/Mn^{3+} ions to maintain charge neutrality. These systems exhibit many significant properties like charge and orbital ordering, metal–insulator transition, ferromagnetic–paramagnetic phase change, magnetoresistance, MCE, spin-glass behavior depending on the charge density, temperature and atomic structure [59,60,61].

Colossal magnetoresistance phenomena were observed in the perovskite-type hole-doped manganites in which the double-exchange ferromagnetic metal phase and the charge–orbital ordered antiferromagnetic phase compete with each other. The chemical randomness or the impurity doping may cause major modifications in the electronic phase diagram as well as in the magnetoelectronic properties. $LaMnO_3$ crystallize in an orthorhombic structure $CaTiO_3$ type Pnma space group. Fig.6.32 showed the crystalline structure of $CaTiO_3$.

6.4.2. Sample preparation

Polycrystalline samples with nominal composition $La_{2/3}Sr_{1/3}Mn_{1-x}Co_xO_3$ (x=0.5, 0.6, 0.7, 0.8, 0.9, 1) were prepared by standard ceramic reaction at high temperatures. The mixtures of the respective oxides were calcinated at 1200ºC and then were pressed and sintered in air at 1300ºC for 24 h. In order to obtain a good homogeneity the samples was several time milled in agate mortar.

6.4.3. Structural characterization of $La_{2/3}Sr_{1/3}Mn_{1-x}Co_xO_3$

The crystal structure was checked by X-ray Diffraction using a Bruker 8 XD diffractometer at the Faculty of Physics, Babes-Bolyai University. XRD was carried out with Cu K_α radiation (λ = 0.15406 nm) at room temperature measured in 2θ = 20° to 70° with a step of 0.1 degree and an acquisition time of 5 seconds in order to increase measurements accuracy.

The X-ray diffraction patterns of $La_{2/3}Sr_{1/3}Mn_{1-x}Co_xO_3$ showed that the compounds are single phases, within the limit of experimental errors. All the compounds crystallize in a rhombohedral structure. The lattice parameters decrease slightly when the Co content increases. The monotonic decrease of the unit cell volume, with increasing cobalt content, indicates a random distribution of the Mn and Co ions in the lattice which means that not exist in long-range Co/Mn order [62].The analysis of diffraction pattern was investigated using the PowderCell software. As example the X-ray diffraction patterns of the $La_{2/3}Sr_{1/3}Mn_{1-x}Co_xO_3$ sample are presented in Fig.27.

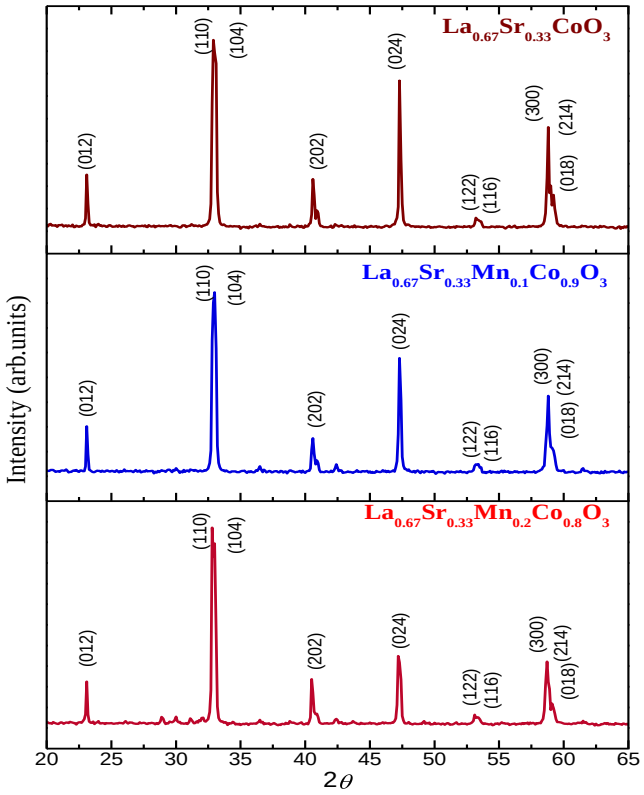

Fig.27. X-ray diffraction patterns of the $La_{2/3}Sr_{1/3}Mn_{1-x}Co_xO_3$ compounds for x=0.8, 0.9, 1

6.4.5. Magnetic properties and magnetocaloric effect of $La_{2/3}Sr_{1/3}Mn_{1-x}Co_xO_3$

An Oxford Instruments MagLab System 2000 was used for magnetization measurements. The samples were studied in magnetic fields up to 5T in the temperature ranges 4.2K–750K. The resistivities were measured in a cryogen-free cryostat CFM-7T (Cryogenic Ltd.) by the four-probe technique. Some magnetization isotherms for the compounds with x=1 is plotted in Fig.28. One can see that the saturation is not attended even in 5T external magnetic field. Similar behaviors were obtained in all cases. In addition, low magnetic hysteretic behavior was found in M(H) curves at low temperatures. The Curie temperatures decrease from 212K at x=1 to 147K at x=0.5. The temperature dependences of magnetic entropy change in 0.5, 1, 3 and 5T external applied fields for the compound with x =1 are plotted in Fig.29. The magnetic entropy changes were determined from magnetization isotherms, between zero field

and a maximum field (H_0) using the thermodynamic relation (5.2) with an increment in temperature between measured magnetization isotherms (ΔT = 5K for our data).

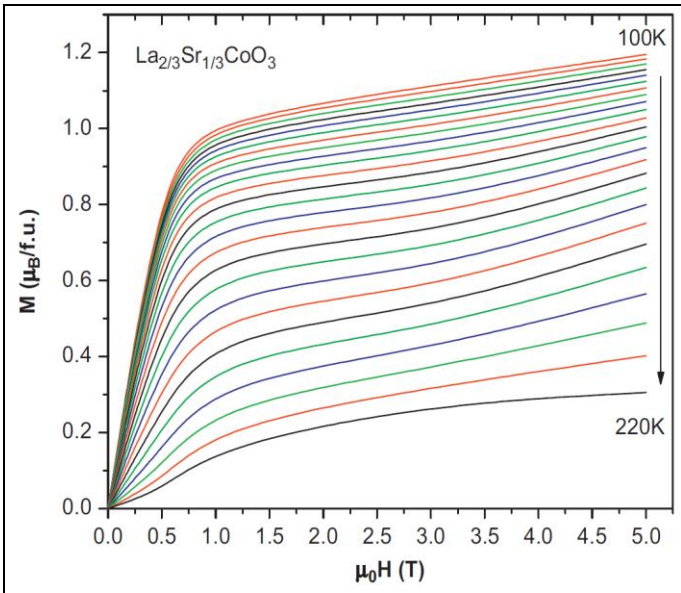

Fig.28. Magnetization isotherms taken around transition temperature for $La_{2/3}Sr_{1/3}Mn_{1-x}Co_xO_3$ *(x=1)*

The maximum values of entropy change occur almost around the transition temperatures for all the compounds. In our case the maximum value is around 1.37J/kgK in a 5 T magnetic field for the compound with x=1. The magnetic entropy change decreases with about 0.6J/kgK in a field of 3T. These values are somewhat smaller than those evidenced in other perovskites but high enough for technical interest.

The magnetic cooling efficiency was evaluated by considering the magnitude of the magnetic entropy change using the relation (5.3). As the most ferromagnetic materials, $La_{2/3}Sr_{1/3}Mn_{1-x}Co_xO_3$ shows a second-order magnetic phase transition. It should be noted that a first-order transition is able to concentrate the MCE in a narrow temperature range, whereas second-order transitions are usually spread over a broad temperature range, which is beneficial for active magnetic refrigeration [63-65].

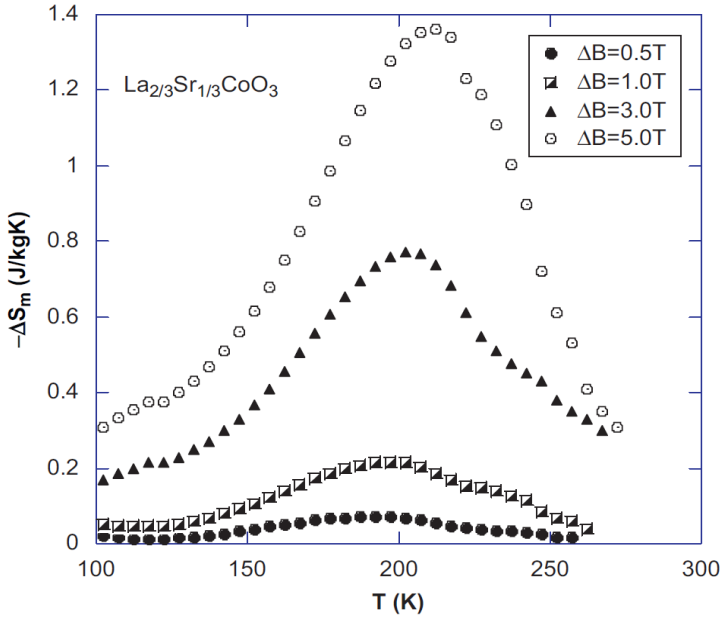

Fig.29. The temperature dependences of the magnetic entropy change for $La_{2/3}Sr_{1/3}Mn_{1-x}Co_xO_3$ *(x=1)*

6.4.6. Preliminary conclusions. The samples were prepared by the conventional ceramic method. X-ray analysis showed the presence of one phase only, in all studied samples. The

lattice parameters decrease slightly when the Co content increases. The Curie temperatures decrease from 212 K at x=1 to 147 K for the sample with x=0.5. At low temperatures low hysteretic behavior was observed. The paramagnetic Curie temperatures for high Co content are negative, suggesting that antiferromagnetic interactions become dominant.

Negative magnetoresistance was evidenced in all cases. The resistivity decreases with increasing Co content, reaching the lowest value for x=1 suggesting the important role of the Co^{3+} subsystem in electrical conduction. The low value of resistivity, in the hightemperature region can be the result of a carrier hopping mechanism together with a charge disproportionation effect of Co^{3+} ions in Co^{2+} and Co^{4+}. The magnetic measurements were performed in a large temperature range, 4.2–750K and external magnetic fields up to 5 T. The maximum magnetic entropy change was obtained for the sample with x=1 in ΔB=5T. The RCP have values comparable with the values obtained in other perovskite-type compounds. The adiabatic magnetic entropy changes, |ΔS|, were determined from magnetization data. Large magnetocaloric effect (MCE) has been obtained in all studied samples. The studied compounds may be considered as magnetic materials operated in the intermediate temperature range.

Conclusions

Samples $\mathbf{Dy_xLa_{1-x}Ni_5}$ was milled at low energy to induce good homogeneity, followed by a high energy milling using the Fritch planetary mill.. This technique follows a good control of stoichiometry with reproducible results. The crystal structure of $Dy_xLa_{1-x}Ni_5$ compounds was checked by X-ray diffraction. The Bragg peaks corresponding to $DyNi_5$ phase are broadened by milling but no additional peaks are observed. In $Dy_xLa_{1-x}Ni_5$ system there is a transition from spin fluctuations behaviour, characteristic for $LaNi_5$, to a ferrimagnetic type ordering for $x \geq 0.2$. The 4f–3d exchange interactions are mediated by R5d band. The Dy5d band polarization is due both to local 4f–5d exchange and 5d–3d and 5d–5d band hybridizations by short range exchange interactions with neighbouring atoms. The mean effective nickel moments decrease when increasing dysprosium. The magnetic behaviour of nickel can be described in the spin fluctuation model. The magnetic entropy change have maximum values around 6J/(kgK) in a 3T external magnetic field [30]. The relative cooling power (RCP) has enough high values to could consider this system for technical applications.

In $\mathbf{Tb_8Co_{16-X}Cu_X}$ compounds with Laves phase structure we have studied the magnetic properties and the magnetocaloric effect. The cobalt behavior in these compounds

can be described as a weak ferromagnet. Partial quenching of spin fluctuation by internal field was observed. Large magnetic entropy changes have been observed for all concentrations. The transition temperature can be tuned via Cu concentration. These suggest that $Tb_8Co_{16-X}Cu_X$ has a potential application as a working substance of magnetic refrigeration in the temperature range 190K-270K [39,40].

In this research, the structural, magnetic and magnetocaloric properties of $Tb_{1-X}Y_XCo_2$ compounds were presented. Some general structural and magnetic properties have been considered for the RM_2 class of intermetallic compounds.

The $\mathbf{Tb_{1-X}Y_XCo_2}$ compounds.with x = 1,2,3,4,5 and 6 were successfully prepared. X-ray diffraction measurements confirm the formation of the cubic $MgCu_2$ (C15) structure in all of the investigated samples. The lattice parameters were found to be little dependent on yttrium content. All of the investigated compounds were found to be ferrimagnetically ordered. The cobalt magnetic moments at 4.2 K were found to decrease with increasing Ycontent. The Curie temperature was found to decrease with increasing Y content. There are local 4f–5d exchange interactions as well as 5d–3d short range interactions with neighboring Co atoms to the Tb one. The variations of cobalt moments, when substituting magnetic Tb by nonmagnetic Y, can be attributed to diminution of the exchange interactions.

The magnetocaloric effect was also studied. The obtained maximum entropy change values were found to decrease from 5.3 J/kgK for x = 1 to 1.9 J/kgK for x = 6 for a magnetic field change from 0 to 4 T. In an external magnetic field change from 0 to 2 T, the magnetic entropy change values were found to decrease to 3.25 J/kgK for x = 1 and 1.2 J/kgK for x = 6 respectively. The decrease of magnetic entropy change with increasing yttrium content may be caused by the decrease in the concentration of Tb^{3+} ions. The large *RCP* values obtained in these materials were mainly attributed to the large δT_{FWHM} values. It was found that $RCP(\Delta S)/\Delta B$ values are quite independent of Y concentration. Due to their high *RCP* values these compounds are promising candidates for applications in magnetic refrigeration devices in the intermediate temperature range.

The samples $\mathbf{La_{2/3}Sr_{1/3}Mn_{1-x}Co_xO_3}$ were prepared by the conventional ceramic method. X-ray analysis showed the presence of one phase only, in all studied samples. The lattice parameters decrease slightly when the Co content increases. The Curie temperatures decrease from 212 K at x=1 to 147 K for the sample with x=0.5. At low temperatures low hysteretic behavior was observed. The paramagnetic Curie temperatures for high Co content are negative, suggesting that antiferromagnetic interactions become dominant.

Negative magnetoresistance was evidenced in all cases. The resistivity decreases with increasing Co content, reaching the lowest value for x=1 suggesting the important role of the Co^{3+} subsystem in electrical conduction. The low value of resistivity, in the high temperature region can be the result of a carrier hopping mechanism together with a charge disproportionation effect of Co^{3+} ions in Co^{2+} and Co^{4+}. The magnetic measurements were performed in a large temperature range, 4.2–750K and external magnetic fields up to 5 T. The maximum magnetic entropy change was obtained for the sample with x=1 in ΔB=5T. The RCP have values comparable with the values obtained in other perovskite-type compounds. The adiabatic magnetic entropy changes, |ΔS|, were determined from magnetization data. Large magnetocaloric effect (MCE) has been obtained in all studied samples. The studied compounds may be considered as magnetic materials operated in the intermediate temperature range.

Selected references

[1] E.Warburg, Ann. Phys. Chem 13 (1881) 141

[2] P.Debye Ann.Physik 81 (1926) 1154

[3] W.F.Giaque, J.Amer.Chem. Soc. 49 (1927) 1864

[4] W.F.Giaque and D.P.MacDougall Phys. Rev. 43 (1933) 768

[5] G.V.Brown, J.Appl.Phys. 47 (1946) 3673

[6] V.K.Pecharrsky and K.A.Gschneider Jr.J.Appl.Phys. 85, 5365 (1999)

[7] K.A.Gschneider Jr. And V.K.Pecharscky, Annu.Rev.Mater.Sci. 30, 387 (2000)

[8] V.K.Pecharscky, K.A.Gschneider Jr., A.O.Pecharscky and A.M.Tishin, Phys. Rev. B 64 (2001) 144406

[9] Felix cassanova PhD thesis universitat de Barcelona 2003

[10] S.Y.Dan`kov, A.M.Thishin, V.K.Pecharsky, and K.A.Gschneidner, Jr., Rev.Sci.Instrum. 68, 2432 (1997)

[11] L.Giudici PhdThesis Politecnici di Torino 2009

[12] B. Bleaney, Proc. Roy. Soc. A 204, 203 (1950).

[13] A.H.Cooke, H.J.Duffus, and W.P.Wolf, Philos. Mag. 44, 623 (1953).

[14] H. Ishimoto, N. Nishida, T. Furubayashi, M. Shinohara, Y. Takano, Y. Miura, and K. Ono, J. Low Temp. Phys. 55, 17 (1984).

[15] *G. Nolze and W. Kraus,* PowderCell 2.3 Program, *BAM Berlin (2000)*

[16] *S. Foner,* Rev. Sci. Instrum. *30, 548–557 (1959)*

[17] P.W. Anderson, Phys. Rev. 124, 41 (1961)

[18] J. Friedel, Can. J. Phys. 34, 1190 (1956); Nuovo Cimento Suppl. 7, 287 (1958)

[19] E Burzo et al 2002 J. Phys.: Condens. Matter 14 8057

[20] V.K. Pecharsky, K.A. Gschneider Jr. Phys. Rev. Lett., 78 (1997), p. 4494

[21] V.K. Pecharsky, K.A. Gschneider Jr. Phys. Rev. Lett., 78 (1997), p. 4494

[22] H.Y. Hwang, S.W. Cheong, P.G. Radaelli, M. Marenzio, B. Batlogg Phys. Rev. Lett., 75 (1995), p. 914

[23] E. Burzo, A. Chelkowski, H. R. Kirchmayr, Landolt Börnstein handbuch, vol. III/19d2, Springer Verlag, (1990)

[24] P. Scherrer, Göt. Nachr. **2**, 98 (1918).

[25] A. Barlet, J. C. Genna, P. Lethuillir, Cryogenics **31**, 801 (1991).

[26] V. I. Anisimov, F. Aryasetiawan, A. I. Lichtenstein, J. Phys.: Condens. Mat. **9**, 767 (1997)

[27] T. Moriya, J. Magn. Magn. Mater. **100**, 201 (1991)

[28] A. Georges, G. Kothar, W. Krauth, M. I. Rosenberg, Rev. Mod. Phys. **68**, 13 (1996)

[29] A. Georges, G. Kothar, W. Krauth, M. I. Rosenberg, Rev. Mod. Phys. **68**, 13 (1996)

[30] E. Burzo, L. Chioncel, E. Dorolti, R. Tetean, A Bezergheanu JOAM Vol. 10, No. 4, April 2008, p. 805 – 808.

[31] H.D. Liu, D.H. Wang, S.L. Tang, Q.Q. Cao, T. Tang, B.X. Gu, Y.W. Du, J. Alloy Compd., **346**, 314, (2002)

[32] H. Wada, S. Tomekawa, M. Shiga, J. Magn. Magn. Mater., **196**/**197**, 689 (1999)

[33] D.H. Wang, S.L. Tang, H.D. Liu, W.L. Gao and Y.W. Du, Intermetallics, **10**, 819 (2002).

[34] E. Gratz and A.S. Markosyan, J. Phys: Condens. Matter, **13**, R385 (2001)

[35] E. Burzo, A. Chelkovski and H. R. Kirchmayr, Landolt Bornstein Handbook, Springer, Berlin, vol **III/19d2** (1990)

[36] K.H.J. Buschow, Rep. Progr. Phys. **40**, 1179 (1977)

[37] K.H.J. Buschow, Rep. Progr. Phys. **40**, 1179 (1977)

[38] E. Burzo, R. Lemaire, Solid State Commun. **84**, 12, 1145 (1992)

[39] E. Brück, M. Ilyn, A.M. Tishin, O. Tegus, J. Magn. Magn. Mater. **290–291,** 8 (2005).

[40] R.Tetean, R.Grasin, ABezergheanu Studia UBB Physica, LVI, 2, p.39, 2011

[41] R.Tetean, E. Burzo, I.G. Deac, J. Alloy. Compd., **442**, 206 (2007)

[42] J. Voiron, A. Berton, J. Chaussy, Phys. Lett. 50A (1974)

[43] W. Steiner, E. Gratz, H. Ortbauer, H.W. Camen, J. Phys. F 8 (1978) 1525

[44] E. Gratz, N. Pillmayr, E. Bauer, G. Hilscher, J. Magn. Magn. Mater. 70 (1987)

[45] N.V. Baranov, A.I. Kozlov, A.N. Pirogov, E.V. Sinitsyn, Sov. Phys. JETP 69 (1989)

[46] N.V. Baranov, A.N. Pirogov, J. Alloys Compounds 217 (1995)

[47] R. Kuentzler, A. Tari, J. Magn. Magn. Mater. 61 (1986)

[48] N. Pillmayr, C. Schmitzer, E. Gratz, G. Hilscher, V. Sechovsky, J. Magn. Magn. Mater. 70 (1987)

[49] G. Hilscher, N. Pillmayr, C. Schmitzer, E. Gratz, Phys. Rev. B 37 (1988) 3480

[50] N.V. Baranov, A.A. Yermakov, A.N. Pirogov, A.E. Teplykh, K. Inoue, Yu. Hosokoshi, Physica B 269 (1999)

[51]][H.M. Rietveld, Journal of Applied Crystallography 2 (1969)

[52] H. Ebert, D. Ködderitzsch and J. Minár, Rep. Prog. Phys. 74 (2011) 096501

[53] S.H. Vosko, L. Wilk and M. Nusair, Can. J. Phys. 58 (1980) 1200

[54] S.H. Vosko, L. Wilk and M. Nusair, Can. J. Phys. 58 (1980) 1200

[55] ref. 7 de la K.W. Zhou,… Solid State Commun., 137

[56] A. Arrott, Phys. Rev. **108**, 1394 ~1957

[57] J. Lyubina, O. Gutfleisch, M. D. Kuz'min, M. Richter, Journal of Magnetism and Magnetic Materials, **320**, 2252-2258, (2008)

[58] J. Lyubina, O. Gutfleisch, M. D. Kuz'min, M. Richter, Journal of Magnetism and Magnetic Materials, **320**, 2252-2258, (2008)

[59] P.G. Radaelli, D.E. Cox, M. Marenzio, S.W. Cheong, P.E. Schiffer, A.P. Ramirez, Phys. Rev. Lett. 75 (1995) 4488.

[60] R. Mahesh, R. Mahendiran, A.K. Raychaudhuri, C.N.R. Rao, J. Solid State Chem. 120 (1995) 204.

[61] R. Mahesh, R. Mahendiran, A.K. Raychaudhuri, C.N.R. Rao, J. Solid State Chem. 120 (1995) 204.

[62] E. Bruck, J. Phys. D: Appl. Phys. (2005) R381.

[63] M.-H. Phan, S.-C. Yu, N.H. Hur, Appl. Phys. Lett. 86 (2005) 072504.

[64] R.Tetean, I.G. Deac, E. Burzo, A. Bezergheanu JMMM 320 (2008) e179–e182